CHAPTER 2

Ruthenium catalyzed benzylic sp^3 C-H oxidation of Dodecahydrotriphenylene

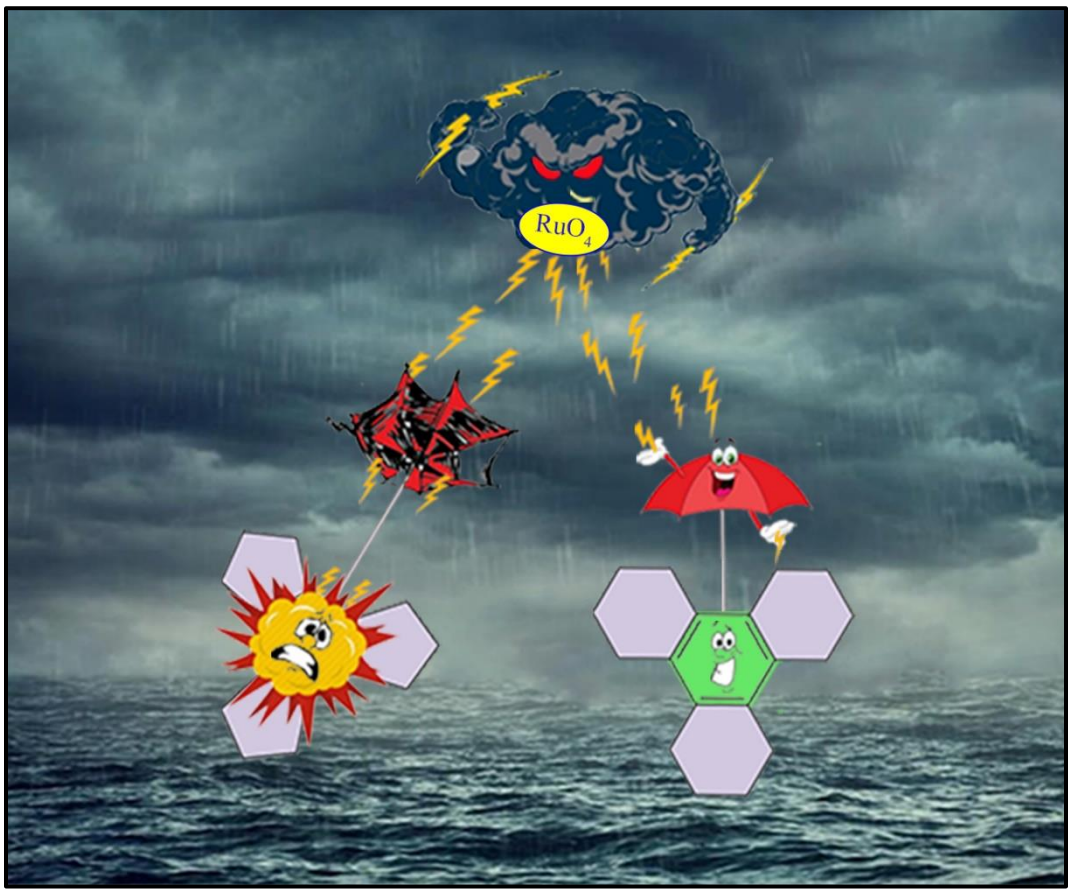

2.1 Abstract

Dodecahydrotriphenylene, a higher homologue of trindane has been found to undergo unidirectional benzylic sp^3 C–H oxidation and the central benzene ring stays intact under identical reaction conditions, unlike trindane. It has been known that ruthenium tetroxide often targets sp^2 C–H site to produce oxidative compounds, however in present case it has been found to produce benzylic ketones *via* sp^3 C–H oxidation. Density functional theory (DFT) calculations have also been carried out to investigate the potential energy, energy barrier and HOMO–LUMO energy gap of the products.

2.2 Introduction

In organic synthesis, selective benzylic oxidation of alkylaromatics is a key technique for the synthesis of aryl ketones.[1-6] Aryl ketones play a vital role in the field of perfumes, flavours, bioactive molecules, and fine-chemical industries.[7, 8]

Alkylarenes, especially polycyclic aromatic hydrocarbons (PAHs) with three branchphenes (i.e. benzocyclotrimers, BCTs) such as trindane **35** and dodecahydrotriphenylene **36** (**Fig. 2.1**) have attracted a lot of significance in fundamental investigations as well as practical applications.

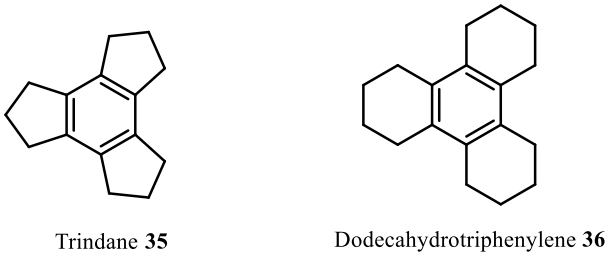

Trindane **35** Dodecahydrotriphenylene **36**

Figure 2.1 Some common alkyl arenes

2.2.1 *Oxidation of alkylarenes*

Various methods have been widely used for the oxidation of alkylarenes. Amongst these, benzylic oxidation of alkylarenes provides valuable synthons that can lead to many natural products, agrochemicals and pharmaceuticals.[8] Additionally, oxidized alkylarenes are widely utilized in organic transformations[9], commercial production of oxygenated compounds[10], preparation of aromatic precursors in the pharmaceutical industry[11, 12] development of advanced materials[13, 14], along with vital intermediates during the synthesis of fine chemicals.[15, 16] There are numerous reagents that have been explored for oxidation like $KMnO_4$, H_2O_2, $NaIO_4$, ozone, mCPBA, iodine(V) species, *tert*-butyl hydroperoxide (TBHP), phenylmethylsulfoxide (PMSO), TEMPO, and hydroxylamine derivatives.[17-23] However, in the traditional alkylarene oxidations,

excessive amounts of oxidizing agents and harsh reaction conditions were needed.[24] The oxidative activation of alkylarenes by transition metal complexes has received a lot of attention.[25]

With the intent of using water as an oxygen supplier for the oxidation, Liu *et al.* have recently reported a palladium-catalyzed oxidation strategy for transforming alkylarenes **57** into aromatic ketones type **58**.[26] Without the need of additional oxidants, various alkylarenes have been selectively oxidized using ^{18}O-labeled water to give corresponding aromatic ketones with only H_2 byproduct. (**Scheme 2.1**)

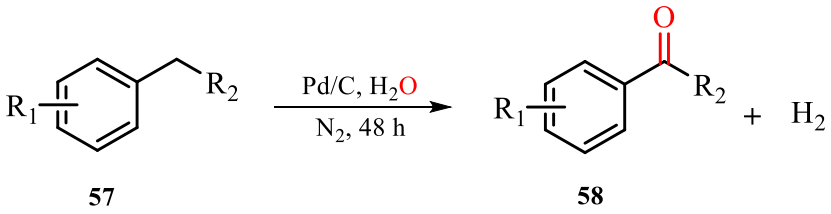

57 **58**

Scheme 2.1 Oxidation of alkylarenes with water as oxygen supplier

Wang *et al.* recently developed a simple approach for chlorine radical-mediated aerobic oxidation of alkylarenes **59** to carbonyl compounds.[27] This procedure used air as a sustainable oxidant and readily available HCl for hydrogen atom transfer. Initially, photo-catalytically generated chlorine radical (Blue LED) underwent HAT with alkylbenzene followed by dechlorinative oxidation to give the desired keto product **60**. (**Scheme 2.2**)

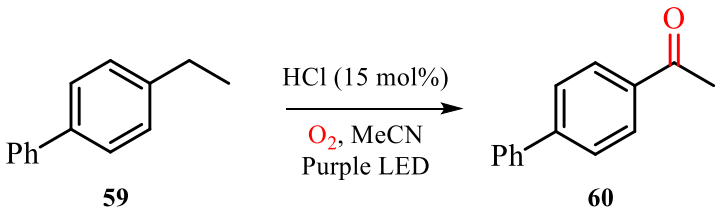

59 **60**

Scheme 2.2 Aerobic oxidation of alkylarenes under LED and air

Selective activation of α-C-H bonds of alkylarenes has attracted a lot of interest from chemist because the selective oxygenation of sp^3 C–H bonds to aromatic ketones is most fundamental transformation that has wide range of application in pharmaceuticals and fine chemicals.[28] For the selective oxidation of alkylarenes, it would be preferable to develop effective heterogeneous catalytic systems. In another approach for aerobic oxidation, NiMn hydrotalcite has been reported to be an effective catalyst in the oxidation of alkylarenes **61** employing molecular oxygen as the only oxidant without any additives.[29] (**Scheme 2.3**) Additionally, they studied how effectively the catalytic system tolerated diverse substrates from various groups and how excellently recyclable it was, holding its structural stability even after several re-uses.

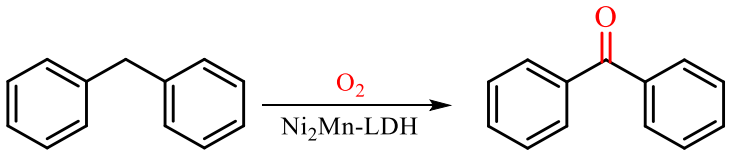

61 Benzophenone **62**

Scheme 2.3 Selective benzylic oxidation of alkylarenes

Sekar *et al.* have developed heterogeneous approach employing readily recoverable and recyclable binaphthyl stabilized Pt-nanoparticles (Pt-BNP) as a catalyst for the selective oxidation of alkylarenes **63** to aromatic ketones **64**.[30] In this oxidation, oxidant TBHP and medium water have been used. (**Scheme 2.4**)

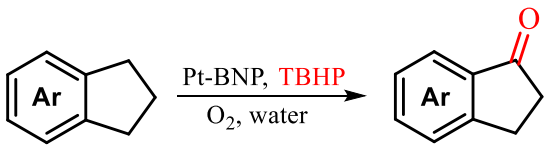

63 **64**

Scheme 2.4 Pt-BNP catalyzed aerobic oxidation of indane **63**

2.2.2 *Selective oxidation using ruthenium catalysts*

There are numerous reports on the selective oxidation of alkylarenes using reagents like $KMnO_4/MnO_2$, ascorbic acid, bismuth-picolinic acid, $NaClO/TEMPO/Co(OAc)_2$, t-BuONa, and o-iodoxybenzoic acid.[31-36] Ruthenium has electron configuration $4d^75s^1$ and it possesses one of highest number of oxidation states in the periodic table ranging from -2 in $Ru(CO)_4^{2-}$ to +8 in RuO_4.[37, 38] Application of ruthenium complexes has significant potential in various catalytic reactions and synthetic approaches. RuO_4 has been extensively utilized among the ruthenium catalysts, as a potent oxidant for oxidative transformation of a variety of organic molecules.[39, 40] RuO_4 can be produced *in situ* by using an oxidant with $RuCl_3$ or RuO_2. The oxidation process may be efficiently carried out in a biphasic system with $RuCl_3$ or RuO_2 and an oxidant like $NaBrO_3$, NaOCl, HIO_4, or $NaIO_4$ etc. (**Fig. 2.2**)

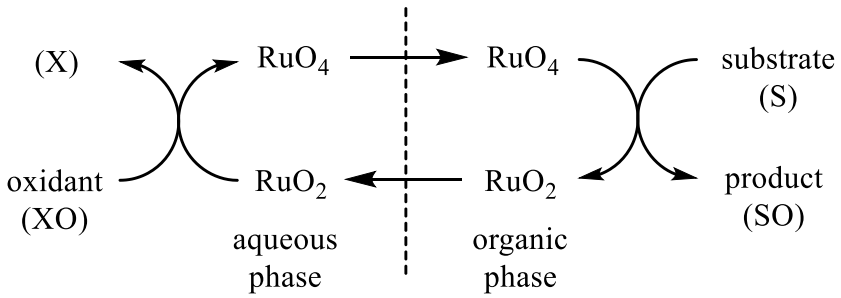

Figure 2.2 General mechanistic pathway to generate RuO_4

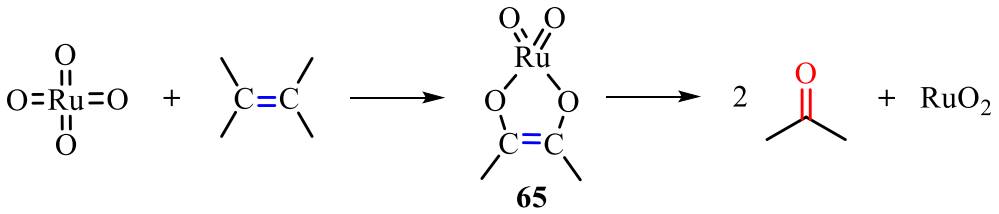

Figure 2.3 Oxidation of olefins into carbonyl compounds using RuO_4

RuO_4 reacts with olefins to produce cyclic ruthenium (VI) diester **65**, which are subsequently broken down into carbonyl compounds by oxidation of the carbon-carbon double bond as per **Fig. 2.3**. Such oxidation requires biphasic CCl_4–H_2O solvent system using catalytic amounts of $RuCl_3$ and $NaIO_4$ oxidant.

The oxidation is often sluggish with carboxylic acids due to inactivation of ruthenium catalysts to form low-valent ruthenium carboxylate complexes. Therefore, several subsequent oxidations have been enhanced by adding CH_3CN into the previous CCl_4–H_2O solvent system.[39] In a typical reaction, the oxidative cleavage of (*E*)-5-decene **66** using a $RuCl_3/NaIO_4$ in a CH_3CN–CCl_4–H_2O solvent system led to 88% yield of pentanoic acid **67**, whereas the same reaction in a traditional CCl_4–H_2O system led to pentanal **68** (17%) along with 80% of the recovered **66**. (**Scheme 2.5**)

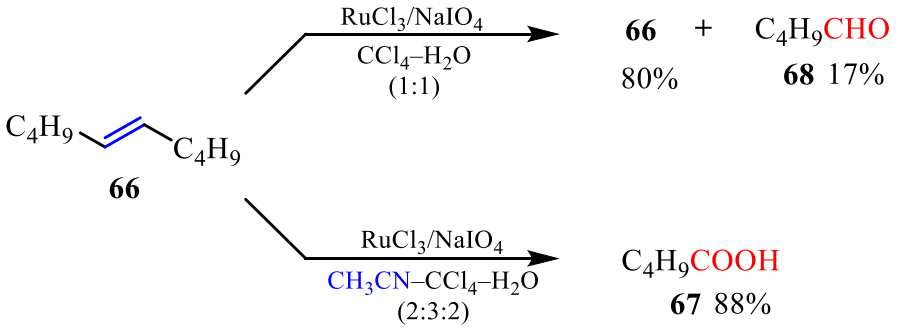

Scheme 2.5 Oxidation process improved by adding CH_3CN in CCl_4–H_2O system

Interestingly under similar reaction conditions a primary alcohol **69** tends to form its corresponding carboxylic acid **70** without affecting the epoxide ring in 75 % yield.[39] (**Scheme 2.6**)

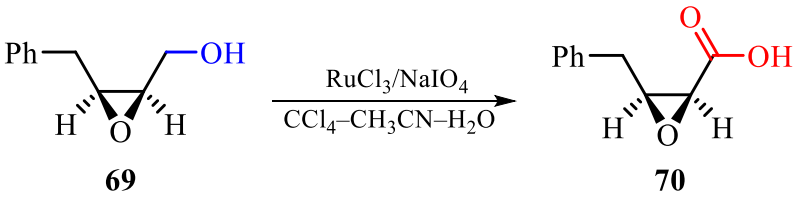

Scheme 2.6 Oxidation of epoxy alcohol **69** to carboxylic acid **70**

Oxidative cleavage of olefins like cyclohexene **71** can result in two different products **72** and **73** by varying the solvent systems as well as oxidant. However, $RuCl_3$ can be converted into RuO_4 using any oxidant like hypochlorite or periodate (**Scheme 2.7**).[41, 42]

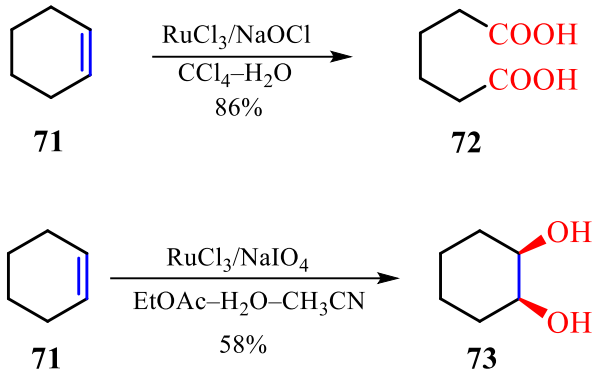

Scheme 2.7 Oxidation of cyclohexene **71**

When considering oxidative ozonolysis, a hazard analysis should be taken into account because it can react with lung surfactants to generate cytotoxic species. Sometimes it can also produce unwanted / unknown oxidative transformation products.[43] This oxidation method is superior to the ozonolysis especially in the degradation of aromatic rings to form carboxylic esters. Some aromatic substrates were subjected to oxidative degradation in the environment of ruthenium tetroxide to form carboxylic acids and esters (**Scheme 2.8**).[44, 45]

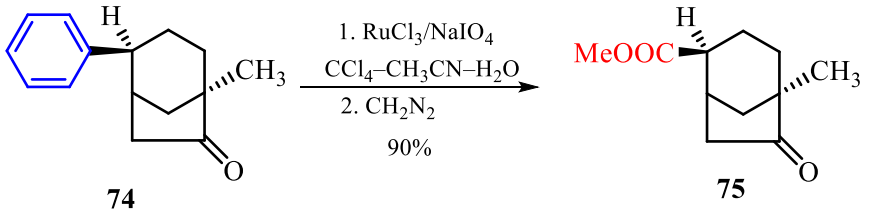

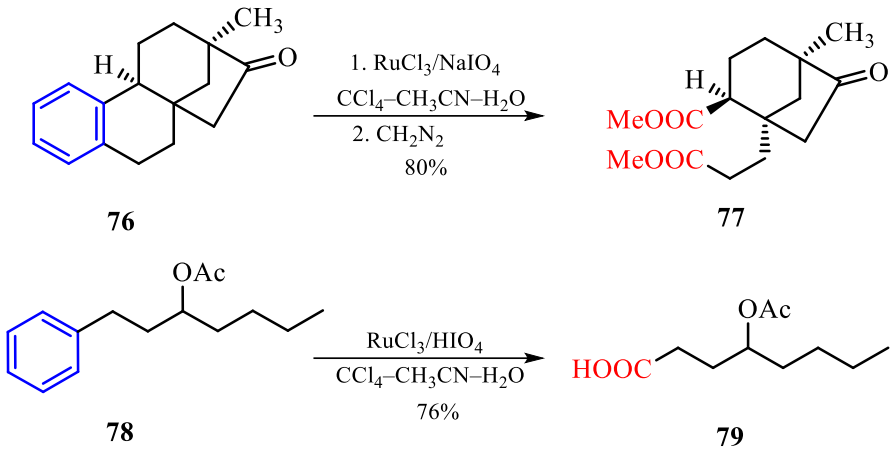

Scheme 2.8 Fate of aromatic rings under oxidative cleavage using Ru

The selective catalytic oxidation of inactive hydrocarbons is still a challenging task in organic synthesis. However, benzylic oxidations of hydrocarbons with ruthenium catalysts using a ligand is quite efficient. Oxidation of hydrocarbons with peroxides such *tert*-BuOOH and peracetic acid in the presence of $RuCl_2(PPh_3)_3$ resulted in the formation of corresponding benzylic ketones. Murahashi *et al.* have successfully employed this method to convert various alkylated arenes **80** into corresponding aryl ketones **81** (**Scheme 2.9**).[46] The $RuCl_2(PPh_3)_3$ / *t*-BuOOH system has the ability to produce a reactive oxo–ruthenium complex *(vide infra)*, which accounts for its remarkable efficacy in oxidizing C-H bonds of alkanes at ambient temperature.

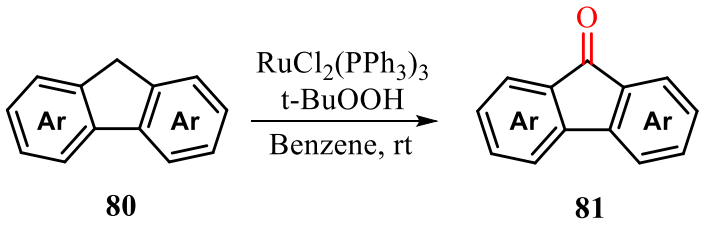

Scheme 2.9 Benzylic oxidation using Ru-ligands as catalysts

Controlling the selectivity in ruthenium catalyzed oxidations is a big challenge. Xiaobing Wan *et al.* have successfully obtained benzylic oxo-products α-diketones **83** using TBHP as an oxidant *via* ruthenium catalyzed alkene oxidation. (**Scheme 2.10**) Their protocol has been reported to have advantages like better functional group tolerance, shorter reaction time, ambient temperatures, ligand-free conditions and practically convenient.[47]

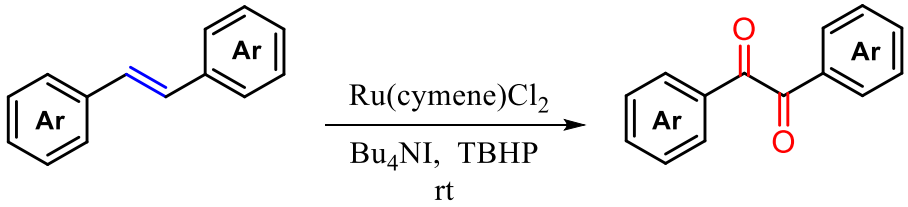

82 **83**

Scheme 2.10 Ru-catalyzed alkenes oxidation to form α-diketones **83**

In summary, it has been observed that Ru-compounds attack alkenes by oxidizing the sp^2 C-H site to produce aryl ketones.[47, 48] Furthermore, it has been shown that $RuCl_3$-$NaIO_4$ has weak reactivity while oxidizing benzylic site of alkylarenes *via* sp^3 C-H activation.[49] Thus, to achieve efficient benzylic sp^3 C-H oxidation of aromatic hydrocarbons to aromatic ketones, ruthenium complexes have been used.[50]

In particular, a hydrocarbon trindane **35** with peripheral methylenes experienced complete degradation in the presence of Ru (VIII) species to yield a fragmented ginkgolide type framework **45**.[51] Instead of triggering benzylic oxidation, ruthenium here vigorously attacked the central benzene ring of trindane **35**. (**Scheme 2.11**)

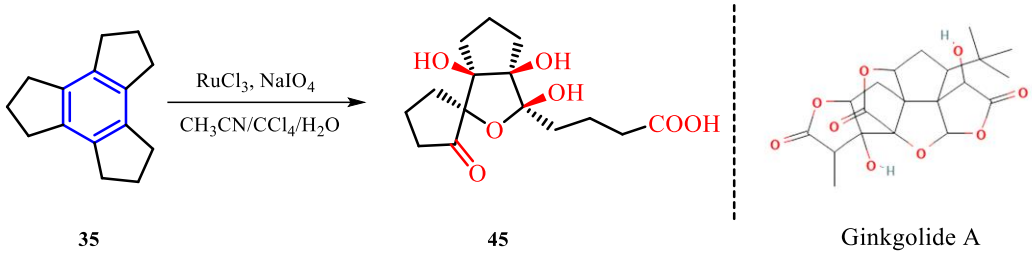

Scheme 2.11 Ru-catalyzed oxidation of trindane **35**

According to the reported plausible route for the conversion, ruthenium species is initially engaged in sp^2 C–H oxidation and then attacks the available double bonds subsequently breaking them apart one by one. (**Scheme 2.12**)

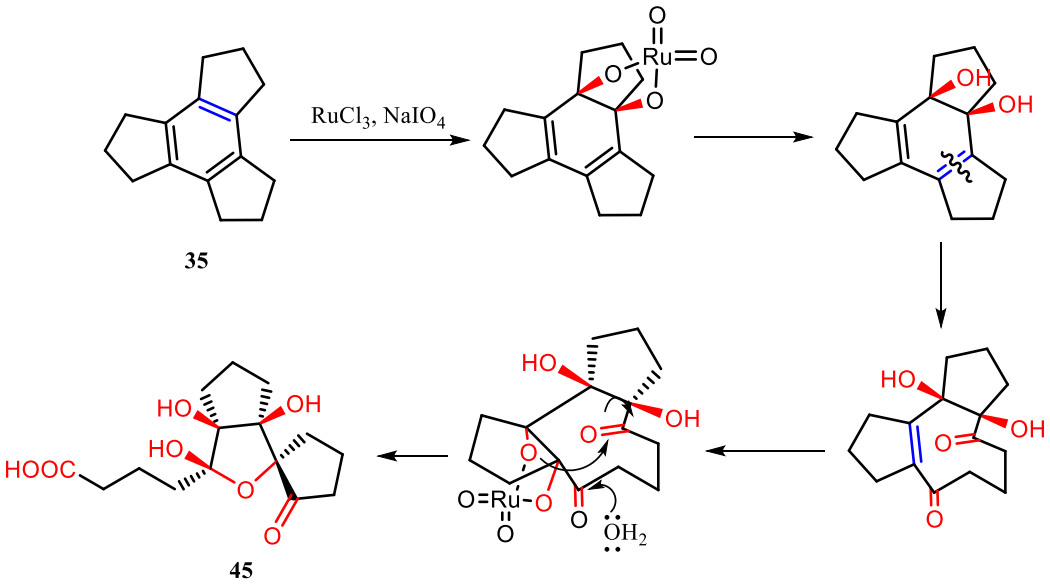

Scheme 2.12 Plausible mechanism of action of Ru (VIII) species on **35**

This one step transformation of trindane **35** into highly oxygenated system prompted us to explore the oxidation of dodecahydrotriphenylene **36** (a higher homologue of **35**).

2.3 Results and Discussion

Initially, dodecahydrotriphenylene **36** was easily assembled quantitatively (~ 60 g) from a single batch *via* cyclotrimerization of cyclohexanone.[52] Thenceforth, we used an aqueous acetonitrile–carbon tetrachloride solvent system to react compound **36** with $RuCl_3$–$NaIO_4$ at room temperature.[39, 53] The reaction was complete after 30 h. (dodecahydrotriphenylene completely consumed, monitored by TLC) Usual workup of the reaction and column chromatography resulted in the ketone **48** accompanying with hitherto unknown ketones **84** and **85** in a total yield of 37%. (**Scheme 1.13**)

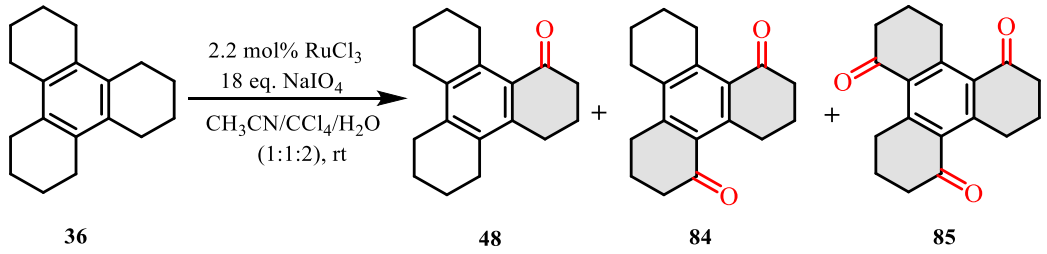

36 **48** **84** **85**

Scheme 2.13 Ru (VIII) mediate oxidation of compound **36**

Table 2.1 Time-dependent study of progress of the reaction

Entry[a]	Reaction time (h)	Yield[b] (%)		
		Compound 48	Compound 84	Compound 85
1	04	22	6	—
2	08	30	9	—
3	12	39	14	—
4	16	33	15	Trace
5	20	30	16	Trace

6	24	22	13	7
7	**30**[c]	**19**	**10**	**8**
8	72[d]	—	—	—
9	96[e]	NR	NR	NR

[a] Compound **36** was taken 5 g for each entry; [b] Isolated yields obtained after column chromatography; [c] Starting material **36** was completely disappeared; [d] Complete degradation of reaction products observed; [e] No reaction (NR) either in presence of $RuCl_3$ alone or $NaIO_4$ alone and unreacted **36** was recovered.

We did a time-dependent investigation of the oxidation by arresting the reaction at various intervals followed by work up and column chromatography of the reaction mixture. Initially formation of decahydrotriphenylen-1-one **48** was observed in the reaction mixture after 3 h, after which the formation of octahydrotriphenylene-1,5-dione **84** (6%) was noticed. The reaction took 20 hours to yield the highest amounts of compound **84** (16%). (**Table 2.1, Figure 2.4**)

Similar to this, hexahydrotriphenylene-1,5,9-trione **85** began to appear in trace amounts after 16 hours of the reaction and then risen substantially and reached to a maximum after 30 hours of the reaction. The products degraded as a result of the prolonged reaction time. For entries **1** to **6**, the unreacted starting material **36** was recovered. (**Table 2.1**)

Moreover, attempts of benzylic oxidation of **36** using $NaIO_4$ alone, in the absence $RuCl_3$ met with no success. Similarly the reaction did not proceed without $NaIO_4$ in the presence of $RuCl_3$ alone demonstrating that the presence of both reagents is essential and that both are participating in the oxidation cycle. It was also observed that with lesser equivalents of $NaIO_4$ or $RuCl_3$ or shorter reaction time, unreacted **36** was isolated.

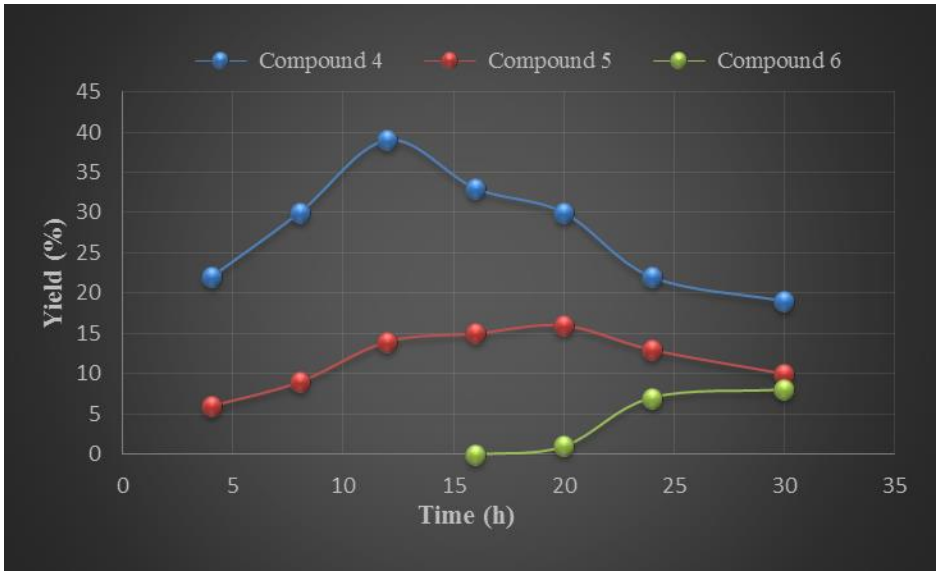

Figure 2.4 Graphical illustration of the reaction time versus yield (%)

The structures of all the synthesized compounds were deduced from their spectral features. The monoketo **48** exhibited a band at 1674 cm^{-1} in its IR spectrum clearly indicates the presence of a conjugated carbonyl group. The ^{1}H NMR (600 MHz, $CDCl_3$) spectrum of **48** displayed a triplet at δ 3.13 for methylene protons adjacent to carbonyl group. Other signals observed at δ 2.78, 2.59, 2.08 and 1.84 for other benzylic and homobenzylic methylene protons. Its ^{13}C NMR (151 MHz, $CDCl_3$) spectrum showed a signal at δ 201.21 indicating the presence of conjugated carbonyl group. In addition signal at δ 141.37, 141.16, 137.13, 134.53, 132.23 and 129.63 confirms the aromatic carbons along with 41.00, 29.70, 27.69, 27.35, 27.24, 26.91, 23.10, 22.77, 22.70, 22.66 for remaining carbons. The structure of **48** was further confirmed by its High Resolution Mass Spectrum (HRMS) which gave a molecular ion peak found at 255.1748 matched with calculated at 255.1749. The spectral features of monoketo **48** is matched with its reported analysis.[54]

The compound **84** gave absorption band at 1684 cm^{-1} for CO group. The ^{1}H NMR of **84** showed two triplet signals at δ 3.29 and 3.16 due to methylene protons next to the carbonyl groups along with signals at δ 2.83, 2.63, 2.15, 2.00 and 1.81

for remaining methylene protons. Its ^{13}C NMR spectrum displayed signal at δ 200.98 for the carbonyl carbon together with signals at δ 148.11, 145.45, 144.95, 134.33, 131.79, 129.67 for aromatic carbons and δ 40.71, 40.51, 30.36, 29.40, 29.18, 27.62, 27.47, 22.76, 22.61, 22.43, 22.27, 22.07 for the leftover methylene carbons. The HRMS of dione **84** gave a molecular ion peak at 269.1521 in contrast to its calculated at 269.1542.

Trione **85** also showed a carbonyl absorption band at 1690 cm^{-1} in its IR spectra, once again confirming to the presence of a conjugated carbonyl group. Interestingly, its proton NMR spectrum of showed only three sets of triplet signals at δ 3.33 for methylenes neighboring to carbonyl group, δ 2.68 for benzylic methylenes and δ 2.05 for other methylene protons. The ^{13}C NMR of **85** showed just one signal at δ 200.12 for three conjugated carbonyl groups, two signals at δ 151.60 and 131.79, indicating the presence of aromatic carbons, and three signals at δ 40.32, 29.81, and 22.44, suggesting the presence of methylene carbons. It is notable to see half number of signals suggesting the C_{3v} symmetry in the molecule. Moreover, its HRMS analysis giving molecular ion peak at 283.1320 whereas calculated was 283.1334.

It is significant to highlight that aforementioned reaction yielded mono, di- and tri-keto derivatives with intact aromatic ring, in contrast to the behavior of trindane **35** that experienced complete oxidative cleavage of the aromatic ring under similar reaction conditions.[51] It is noteworthy to highlight that all of the compounds have been found to be the end result of benzylic sp^3 C–H oxidation. Additionally, it turns out that none of the six homobenzylic sites for compound **36** underwent the oxidation. Moreover, the structure of dione **84** and trione **85** seem to have a *unidirectional character*, with all of the keto groups oriented either clockwise or anticlockwise. Also, compound **36** has six benzylic sites, but only three of them are *chemoselectively* oxidized. (**Scheme 1.13**)

The C_{2v} symmetric diones (**86**, **87** and **88**) as well as the unsymmetrical triones (**89**, **90** and **91**) that may have been produced by further oxidiation of diones were not observed at all. (**Fig. 2.5**)

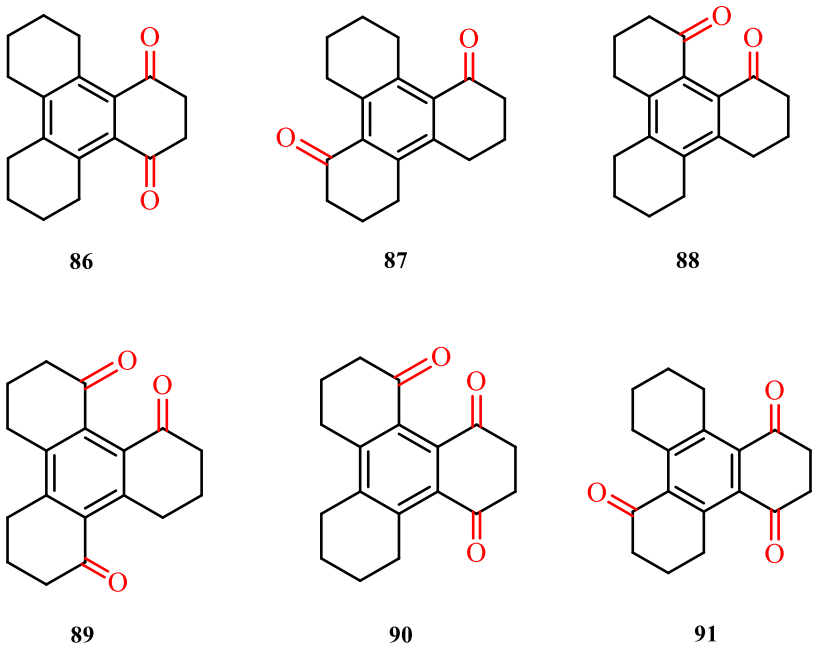

Figure 2.5 Other possible benzylic diones (**86-88**) and triones (**89-91**)

It was also noteworthy to find that the oxidation did not yield the expected fragmented product of the type **92** as observed in the reaction of trindane **35** under similar conditions as reported by S. Ranganathan *et al*. (**Scheme 2.14**)

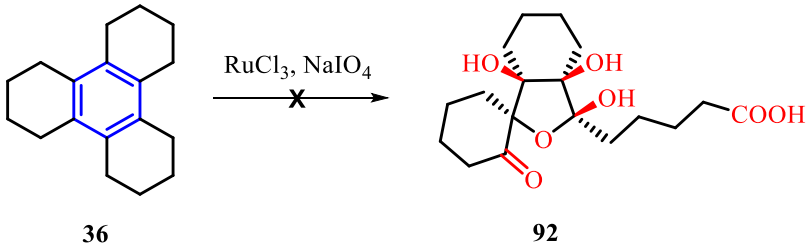

Scheme 2.14 Expected highly oxygenated ring-opened product **92**

It is known that the oxidation of $RuCl_3$ to ruthenium tetroxide takes place *in situ* with the oxidants like periodate or hypochlorite.[55] The folded peripheral cyclohexene rings in compound **36** provide steric hindrance to the ruthenium

tetroxide possibly preventing the attack of the oxidant into the central benzene ring redirecting the reagent to consequent attack on the benzylic sp^3 C–H positions. (**Fig. 2.6**)

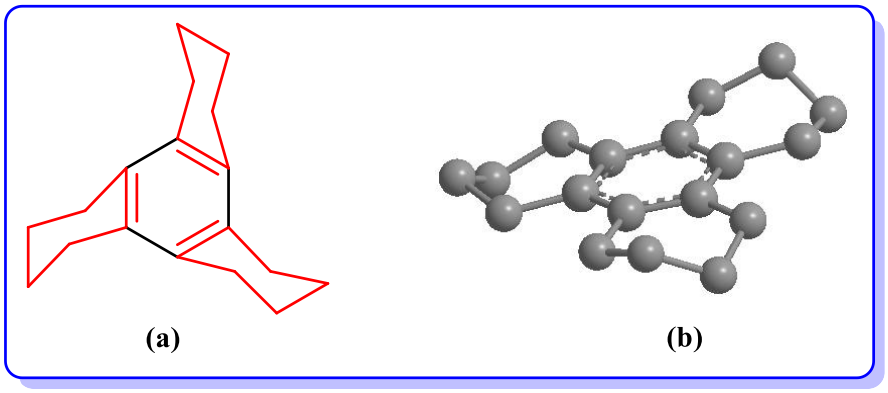

Figure 2.6 a) Folded peripheral cyclohexene rings; **b)** Minimized energy structure of **36** by Chem3D

Ruthenium is used more frequently than osmium in oxidations due to its lower toxicity and isoelectronic relation with osmium.[56, 57] A plausible, concise reaction mechanism for this catalytic oxidation has been proposed. (**Fig. 2.7** and **2.8**) Initial benzylic hydrogen abstracted by *in situ* generated RuO_4 **97** results in the formation of a corresponding free radical, which upon interaction with water, produces an alcohol of the type **93** and forms Ru-oxo/hydroxo species **94**.[49] The subsequent oxidation of **93** through intermediate **95** resulted in the synthesis of a ketone **48**, and produces monooxoruthenium (IV) species **96**, which is eventually oxidized back to RuO_4 **97** by the oxidant periodate for the next redox cycle.[55] Simultaneously in the final step, periodate gets reduced to iodate.

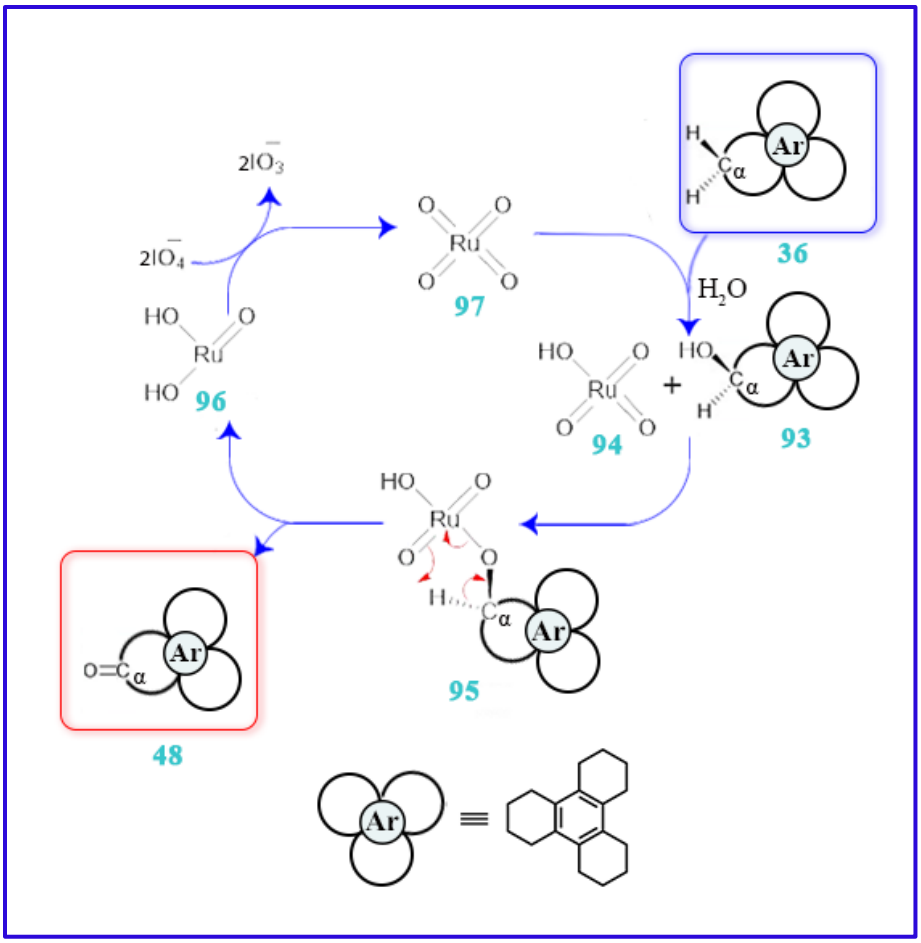

Figure 2.7 Plausible mechanism of action of Ruthenium catalyst

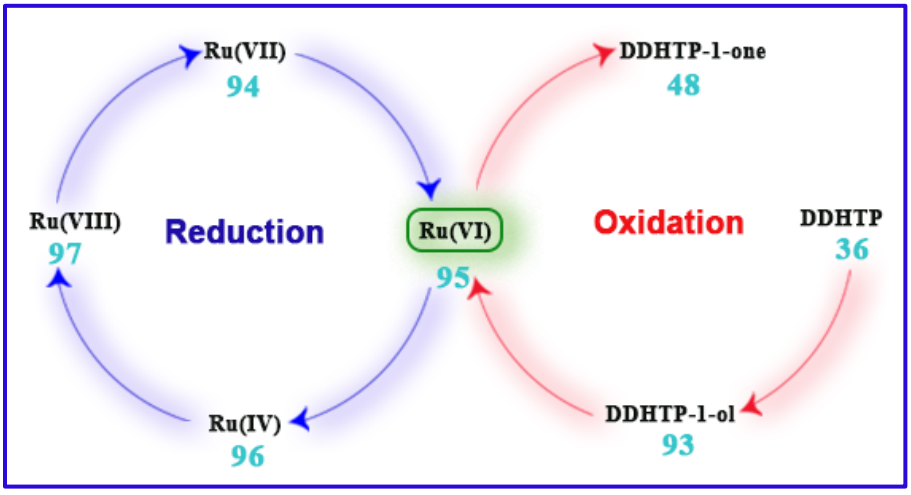

Figure 2.8 A catalytic oxidation-reduction cycle of Ru-oxidation

Fig. 2.9 compares ruthenium assisted various oxidations along with our present work. α-Diketones were produced when activated double bond of alkene is oxidized by the ruthenium catalyst via a sp^2 C–H oxidation process.[47] Complexes of ruthenium with ligands are often used to accomplish benzylic sp^3 C–H oxidation of alkylarenes.[49] The central benzene ring of trindane **35** is completely oxidized when Ru (VIII) species was introduced, resulting in a polycyclic oxygenated product. Interestingly, sp^3 C–H oxidation is not observed in **35** despite the resemblance between **35** and **36**.[51] Nevertheless, we discovered that the core benzene ring in compound **36** is remains intact and that three of the six benzylic sites were chemoselectively oxidized to produce compound **85**, a C_{3v} symmetric keto derivative with *unidirectional character*, along with compounds **48** and **84**.[58]

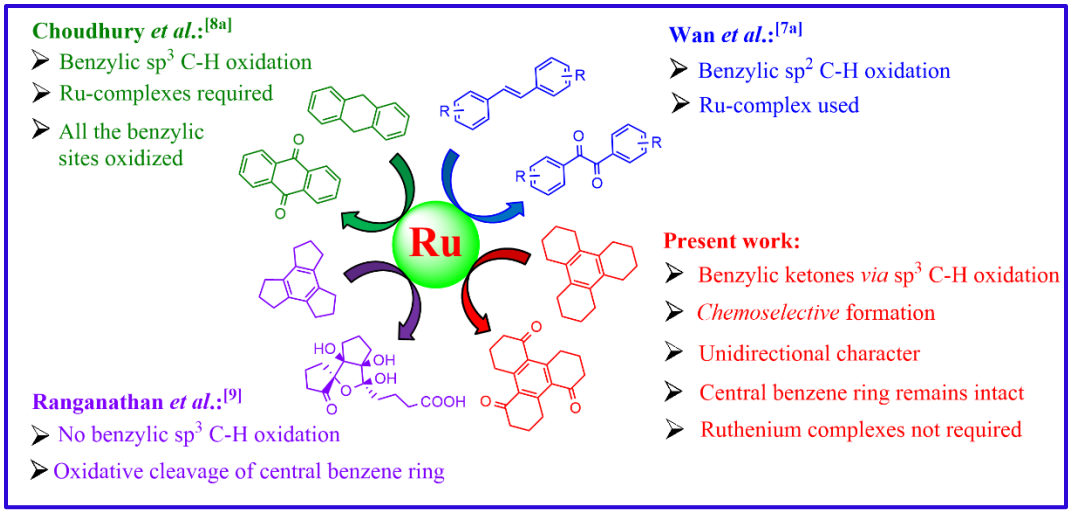

Figure 2.9 An overview of ruthenium mediated oxidations

2.4 Density Functional Theory (DFT) Calculations

We analyzed independent structural optimization to ascertain the minimum energy of each possible isomers of diones (**84, 86-88)** and triones (**85, 89, and 90**). The Gaussian09 software was used for further calculations, including ground-state

structural and electronic (HOMO-LUMO) computations, applying DFT.[59] To precisely anticipate the minimum energy states, the LanL2DZ basis-set for Ru-based systems and the 6-311G basis-set for the other systems combined have been used with the Becke three parameters hybrid functional with Lee-Yang-Perdew correlation functionals (B3LYP).[60] The HOMO-LUMO gap has also been investigated since it conveys vital information like electronegativity (χ), electrophilicity index (ω), global hardness (η), global softness (*S*), chemical potential (μ) etc. We have also independently calculated and optimized the structural geometries using the aforementioned parameters in order to verify the experimental results and comprehend the atomic level properties. In **Fig. 2.10**, the optimized geometries and energies are summarized.

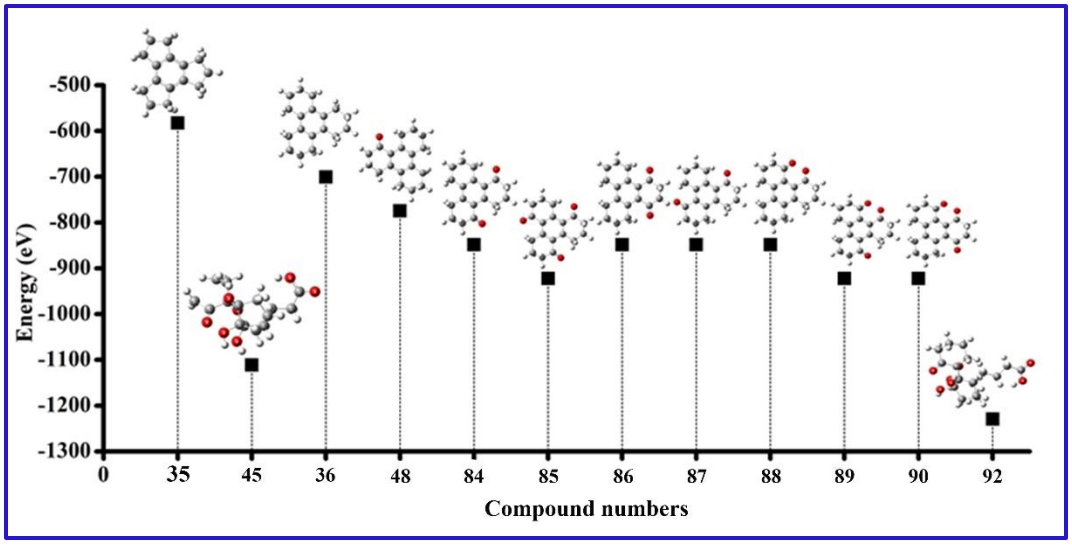

Figure 2.10 Molecules with optimized geometries that reflect their energy state

The molecules **48**, **84**, and **85** are observed to have the least energies compare to all those possible diones and triones (**86-90**), which is also seen in experimental results. This figure displays the DFT-calculated optimized geometry that represented the energy of molecules. Computed potential energies for compounds **48**, **84**, and **85** are -774.392 eV, -848.401 eV, and -922.410 eV,

respectively. Among other prevalent oxidation states of ruthenium, Ru (VIII) is known to be the most stable.[61] The most common Ru(IV) oxidation state is produced by continuous reduction of Ru(VIII), *via* ruthenate(VI) as an intermediary state.

For each step, we computed the relative energy pathway as well as energy barrier and plotted the energy diagram. (**Fig. 2.11**) RuO_4 first eliminates a hydrogen from **36**, which leads its reduction into Ru (VII) and the simultaneous formation of the hydroxy derivative (**IM 93**). For this step, the computed energy barrier is -0.036 keV per atom. Following this, **IM 93** and Ru (VII) species combine to form alkoxyruthenium (VI) (**IM 95**), which has an energy barrier of -0.144 keV per atom. In the key step, the cleavage of the ruthenium-oxygen bond triggers the formation of the keto products **48**, **84**, **85** and the generation of Ru (IV) species. This final step has an energy barrier of 0.12 keV per atom.

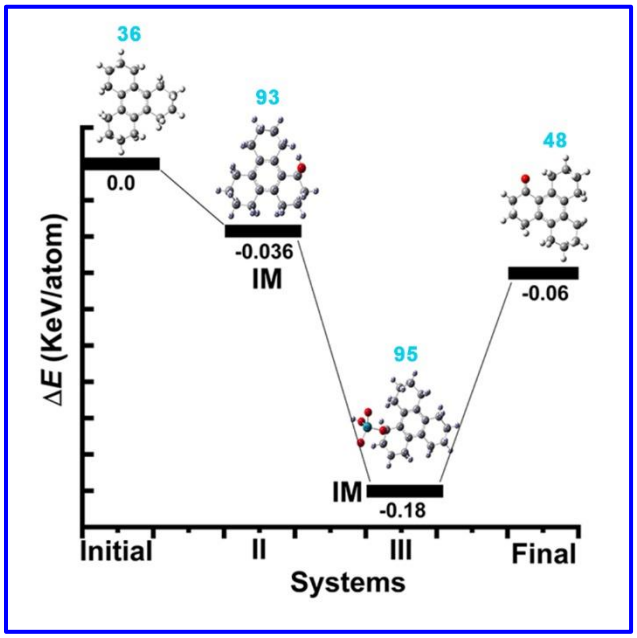

Figure 2.11 Relative energy pathway calculations for the intermediates (IM) throughout the oxidation reaction

2.5 Experimental section

2.5.1 *General information*

All the chemicals were obtained from Sigma Aldrich, SD Fine-Chem Limited and Spectrochem. Hindustan Platinum Pvt Ltd from Navi Mumbai and Heraeus Pvt Ltd from Jaipur have provided gift samples of Ruthenium trichloride ($RuCl_3$). Zirconium tetrachloride ($ZrCl_4$) was purchased from Aldrich. All the solvents were purified by distillation prior to use and stored over oven-dried molecular sieves. Acme's silica gel (60-120 mesh size) was used for column chromatography and mixtures of light petroleum (60-80) and ethyl acetate were used for the elution process. Glass plates were used for the thin layer chromatography (TLC) analysis, with silica gel G containing 13% calcium sulphate as a binder or performed on silica gel aluminium plates. The melting points of all synthesized compounds were recorded under optical Polarized Light Microscope attached with Nikon camera and Linkam heating stage. The spots were observed using iodine vapour or UV light. IR spectra were captured using a SHIMADZU FTIR-245068 spectrophotometer over potassium bromide pellets. The ^{1}H and ^{13}C NMR spectra were recorded using the Bruker Avance (400/500/600 MHz) NMR. The multiplicities of signals in PMR data are assigned by the following abbreviations; singlet as (s), doublet as (d), triplet as (t), quartet as (q), quintet as (quint.), multiplet as (m) and coupling constants (*J*) are designated in hertz. The XEVO G2-XS QTOF Mass Spectrometer from IIT Ropar was used to record the HRMS data of the final compounds.

2.5.2 *Procedure for the synthesis of dodecahydrotriphenylene* **36**

The following literature procedure was used to synthesize compound **36**.[52] A mixture of cyclohexanone (1160.00 mmol, 120.0 mL) and zirconium tetrachloride (46.40 mmol, 10.8 g) was taken in a round-bottomed flask (250 mL) equipped with a condenser. The reaction mixture was refluxed for 10 hours, following which it became orange semisolid. Then it was diluted with chloroform,

and the inorganic salt was filtered off. The filtrate was concentrated under reduced pressure and residual was repeatedly washed with ethanol. The precipitate was collected and dried to obtain a white powder (56.8 g, 62 %). In order to further purify the white powder, it was then recrystallized with $CHCl_3$ / EtOH.

1,2,3,4,5,6,7,8,9,10,11,12-dodecahydrotriphenylene **36**

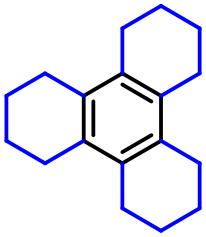

White solid, 58.8 g, 62 % yield, mp 231 °C[52], R*f*: 0.8 (5:0, Pet. Ether:EtOAc); **IR (KBr, cm^{-1})** 2922, 1444, 1259; **^{1}H NMR (400 MHz, $CDCl_3$)** δ 2.82 – 2.42 (m, 1H), 1.82 (ddt, 1H); **^{13}C NMR (101 MHz, $CDCl_3$)** δ 132.68, 26.90, 23.15

2.5.3 *Procedure of $RuCl_3$-$NaIO_4$ oxidation*

After stirring a mixture of sodium metaperiodate (80.2 g, 375.00 mmol) in distilled water (100.0 mL), ruthenium trichloride (125.0 mg, 0.60 mmol) in acetonitrile and carbon tetrachloride (50.0 mL each) was added. Dodecahydrotriphenylene **36** (5.0 g, 20.83 mmol) was added to this mixture, which was then stirred in a vortex for 30 hours at room temperature. The reaction mixture was filtered once the reaction was completed (TLC), and the filtrate was extracted with ethyl acetate (3 x 60 mL). The combined organic extracts were washed with 50 mL of water and 50 mL of brine before being dried over anhydrous sodium sulphate. By removing the solvent at reduced pressure, a dark brown, thick liquid was obtained, which was then chromatographed on a silica gel column using light petroleum and ethyl acetate.

3,4,5,6,7,8,9,10,11,12-decahydrotriphenylen-1(*2H*)-one **48**

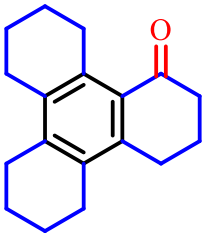

White solid; 1.05 g; 19% yield, mp 225 °C[54], R*f*: 0.6 (4.5:0.5, Pet. Ether:EtOAc); **IR (KBr, cm^{-1})** 2918, 2857 and 1674; **^{1}H NMR (600 MHz, CDCl$_3$):** δ 3.13 (t, J = 6.0 Hz, 1H), 2.78 (t, *J* = 5.9 Hz, 1H), 2.59 (dd, *J* = 14.3, 7.5 Hz, 4H), 2.08 (dd, *J* = 12.8, 6.5 Hz, 1H), 1.84 – 1.66 (m, 4H); **^{13}C NMR (151 MHz, CDCl$_3$):** δ 201.23, 141.38, 141.17, 137.14, 134.54, 132.24, 129.64, 41.01, 29.70, 27.69, 27.36, 27.24, 26.92, 23.11, 22.77, 22.70, 22.66, 22.54; **HRMS (ESI)** *m/z* calculated for $C_{18}H_{23}O$ $[M+H]^+$: 255.1749, found 255.1748

3,4,7,8,9,10,11,12-octahydrotriphenylene-1,5(*2H*,*6H*)-dione **84**

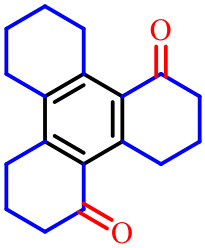

Light yellow solid; 0.52 g; 10% yield, mp 215 °C, R*f*: 0.4 (4.5:0.5, Pet. Ether:EtOAc); **IR (KBr, cm^{-1})** 2934, 2863 and 1684; **^{1}H NMR (600 MHz, CDCl$_3$)** δ 3.29 (t, *J* = 6.0 Hz, 2H), 3.16 (t, *J* = 6.2 Hz, 2H), 2.83 (q, *J* = 5.9 Hz, 3H), 2.63 (dt, *J* = 14.3, 6.1 Hz, 7H), 2.15 – 2.08 (m, 3H), 2.00 – 1.94 (m, 2H), 1.81 (dd, *J* = 11.5, 5.6 Hz, 2H); **^{13}C NMR (151 MHz, CDCl$_3$)** δ 200.99, 200.62, 148.12, 145.46, 144.96, 134.34, 131.80, 129.68, 40.71, 40.51, 30.36, 29.19, 27.62, 27.47, 22.76, 22.61, 22.43, 22.07; **HRMS (ESI)** *m/z* calculated for $C_{18}H_{21}O_2$ $[M+H]^+$: 269.1542, found 269.1521

3,4,7,8,11,12-hexahydrotriphenylene-1,5,9(*2H*,*6H*,*10H*)-trione **85**

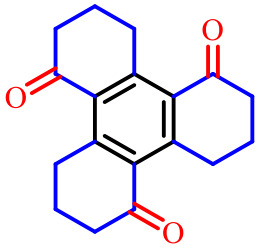

Pale yellow solid; 0.46 g; 8% yield, mp 210 °C, R*f*: 0.5 (4:1, Pet. Ether:EtOAc); **IR (KBr, cm^{-1})** 2868, 1690; **^{1}H NMR (600 MHz, CDCl$_3$)** δ 3.33 (t, *J* = 6.1 Hz, 1H), 2.68 (t, *J* = 6.8 Hz, 1H), 2.05 – 1.99 (m, 1H); **^{13}C NMR (151 MHz, CDCl$_3$)** δ 200.13, 151.62, 131.81, 40.32, 29.82, 22.44; **HRMS (ESI)** *m/z* calculated for $C_{18}H_{19}O_3$ $[M+H]^+$: 283.1334, found 283.1320

2.6 Conclusions

In conclusion, it is found that ruthenium has no impact on the central benzene ring of DDHTP and as an outcome, sp^3 C–H benzylic oxidation resulting in the formation of benzylic ketones **48, 84** and **85** is observed. The table below compiles the distinctiveness of our oxidation in contrast to other ruthenium catalyzed oxidations. Our experimental results and the DFT computations show excellent agreement.

Other Ru oxidations	**Ranganathan's oxidation**	**Our oxidation**
Controlling selectivity is a big challenge due to the involvement of various high-valent Ru species during the oxidation. Hence, complexes using various ligands with Ru are employed to achieve selective benzylic sp^3 C-H oxidations.	Ru(VIII) species vigorously attacks on the central benzene ring of trindane to form ring-opened product.	Selective benzylic sp^3 C-H oxidation leading to formation of ketones (mono, di-, tri-) is observed without employing a Ru-complex. No ligands are require to control the selectivity of oxidation.

Ruthenium attacks *all* the benzylic C-H positions that are available in the molecule to form oxidative products.	No benzylic oxidation occurs.	Benzylic sp^3 C-H oxidation wherein three positions out of six are *chemoselectively* oxidized to form keto derivatives having unidirectional character.
Benzylic α-diketones are formed *via* sp^2 C-H oxidation using Ru-catalyst, in which the catalyst attacks the activated double bond of an alkene.	There is availability of double bonds in the central benzene ring of trindane which undergoes complete oxidative cleavage to give a polycyclic oxygenated product.	Despite the availability of double bonds in the central benzene ring, oxidation occurs at benzylic sp^3 C-H position which is contrary to the behavior of ruthenium tetroxide. The central benzene ring remains *intact* and it forms C_{3v} symmetrical product along with mono and di-keto derivates. This may be due to the steric hindrance of the folded peripheral cyclohexene rings in dodecahydrotriphenylene.
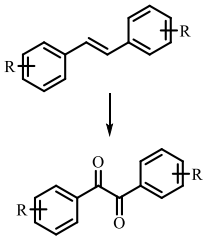 sp^2 C-H oxidation	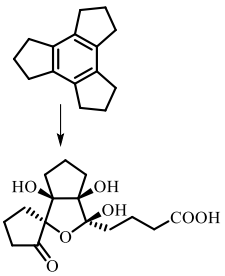 sp^2 C-H oxidation	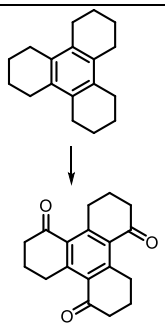 sp^3 C-H oxidation

2.7 References

[1] P. Thansandote, M. Lautens, *Chemistry – A European Journal* **2009**, *15*, 5874-5883.

[2] R. Jazzar, J. Hitce, A. Renaudat, J. Sofack-Kreutzer, O. Baudoin, *Chemistry – A European Journal* **2010**, *16*, 2654-2672.

[3] R. Giri, B.-F. Shi, K. M. Engle, N. Maugel, J.-Q. Yu, *Chemical Society Reviews* **2009**, *38*, 3242-3272.

[4] L. Ackermann, R. Vicente, A. R. Kapdi, *Angewandte Chemie International Edition* **2009**, *48*, 9792-9826.

[5] M. M. Díaz-Requejo, P. J. Pérez, *Chemical Reviews* **2008**, *108*, 3379-3394.

[6] D. Alberico, M. E. Scott, M. Lautens, *Chemical Reviews* **2007**, *107*, 174-238.

[7] C. K. P. Neeli, A. Narani, R. K. Marella, K. S. Rama Rao, D. R. Burri, *Catalysis Communications* **2013**, *39*, 5-9.

[8] H. Hussain, I. R. Green, I. Ahmed, *Chemical Reviews* **2013**, *113*, 3329-3371.

[9] A. Aguadero, H. Falcon, J. M. Campos-Martin, S. M. Al-Zahrani, J. L. G. Fierro, J. A. Alonso, *Angewandte Chemie International Edition* **2011**, *50*, 6557-6561.

[10] S. Zuo, J. Liu, A. Zuo, *Journal of Heterocyclic Chemistry* **2020**, *57*, 2634-2639.

[11] R. Maiti, B. R. Mishra, J. Jowhar, D. Mohapatra, S. Parida, D. Bisoi, *Clinical psychopharmacology and neuroscience : the official scientific journal of the Korean College of Neuropsychopharmacology* **2017**, *15*, 170-176.

[12] K. D. Hargrave, F. K. Hess, J. T. Oliver, *Journal of Medicinal Chemistry* **1983**, *26*, 1158-1163.

[13] L. Zhang, W. Wu, Y. Zhong, S. Zhu, Z. Wang, Z. Zou, *RSC Advances* **2015**, *5*, 87609-87615.

[14] C.-H. Chen, C.-H. Lin, J.-M. Hon, M.-W. Wang, T.-Y. Juang, *Polymer* **2018**, *154*, 35-41.

[15] F. Rong, S. Chow, S. Yan, G. Larson, Z. Hong, J. Wu, *Bioorganic & Medicinal Chemistry Letters* **2007**, *17*, 1663-1666.

[16] J. A. Lessa, I. C. Mendes, P. R. O. da Silva, M. A. Soares, R. G. dos Santos, N. L. Speziali, N. C. Romeiro, E. J. Barreiro, H. Beraldo, *European Journal of Medicinal Chemistry* **2010**, *45*, 5671-5677.

[17] J.-W. Yu, S. Mao, Y.-Q. Wang, *Tetrahedron Letters* **2015**, *56*, 1575-1580.

[18] R. Mayilmurugan, H. Stoeckli-Evans, E. Suresh, M. Palaniandavar, *Dalton Transactions* **2009**, 5101-5114.

[19] C. Miao, H. Zhao, Q. Zhao, C. Xia, W. Sun, *Catalysis Science & Technology* **2016**, *6*, 1378-1383.

[20] M. S. Yusubov, V. N. Nemykin, V. V. Zhdankin, *Tetrahedron* **2010**, *66*, 5745-5752.

[21] B. Karami, M. Montazerozohori, in *Molecules, Vol. 11*, **2006**, pp. 720-725.

[22] S. J. Singh, R. V. Jayaram, *Catalysis Communications* **2009**, *10*, 2004-2007.

[23] A. M. Khenkin, R. Neumann, *Journal of the American Chemical Society* **2002**, *124*, 4198-4199.

[24] C. Zhang, P. Srivastava, K. Ellis-Guardiola, J. C. Lewis, *Tetrahedron* **2014**, *70*, 4245-4249.

[25] J.-B. Feng, X.-F. Wu, *Applied Organometallic Chemistry* **2015**, *29*, 63-86.

[26] J. Zhang, J. Du, C. Zhang, K. Liu, F. Yu, Y. Yuan, B. Duan, R. Liu, *Organic Letters* **2022**, *24*, 1152-1157.

[27] K. Niu, X. Shi, L. Ding, Y. Liu, H. Song, Q. Wang, *ChemSusChem* **2022**, *15*, e202102326.

[28] P. Hu, M. Tan, L. Cheng, H. Zhao, R. Feng, W.-J. Gu, W. Han, *Nature Communications* **2019**, *10*, 2425.

[29] A. Wang, W. Zhou, Z. Sun, Z. Zhang, Z. Zhang, M. He, Q. Chen, *Molecular Catalysis* **2021**, *499*, 111276.

[30] R. Saha, G. Sekar, *Applied Catalysis B: Environmental* **2019**, *250*, 325-336.

[31] F.-L. Zeng, X.-L. Chen, S.-Q. He, K. Sun, Y. Liu, R. Fu, L.-B. Qu, Y.-F. Zhao, B. Yu, *Organic Chemistry Frontiers* **2019**, *6*, 1476-1480.

[32] K.-J. Liu, T.-Y. Zeng, J.-L. Zeng, S.-F. Gong, J.-Y. He, Y.-W. Lin, J.-X. Tan, Z. Cao, W.-M. He, *Chinese Chemical Letters* **2019**, *30*, 2304-2308.

[33] K.-J. Liu, Z. Wang, L.-H. Lu, J.-Y. Chen, F. Zeng, Y.-W. Lin, Z. Cao, X. Yu, W.-M. He, *Green Chemistry* **2021**, *23*, 496-500.

[34] J.-S. Li, F. Yang, Q. Yang, Z.-W. Li, G.-Q. Chen, Y.-D. Da, P.-M. Huang, C. Chen, Y. Zhang, L.-Z. Huang, *Synlett* **2017**, *28*, 994-998.

[35] C. Jin, L. Zhang, W. Su, *Synlett* **2011**, *2011*, 1435-1438.

[36] Y. Bonvin, E. Callens, I. Larrosa, D. A. Henderson, J. Oldham, A. J. Burton, A. G. M. Barrett, *Organic Letters* **2005**, *7*, 4549-4552.

[37] F. A. Cotton, G. Wilkinson, C. A. Murillo, M. Bochmann, *Advanced inorganic chemistry*, 4th ed., John Wiley and Sons, Inc., **1999**.

[38] E. A. Seddon, K. R. Seddon, *The Chemistry of Ruthenium*, Elsevier, **1984**.

[39] P. H. J. Carlsen, T. Katsuki, V. S. Martin, K. B. Sharpless, *The Journal of Organic Chemistry* **1981**, *46*, 3936-3938.

[40] J.-E. Bäckvall, *Modern oxidation methods*, 2nd ed., John Wiley & Sons, **2011**.

[41] T. K. M. Shing, V. W. F. Tai, E. K. W. Tam, *Angewandte Chemie International Edition in English* **1994**, *33*, 2312-2313.

[42] S. Wolfe, S. K. Hasan, J. R. Campbell, *Journal of the Chemical Society D: Chemical Communications* **1970**, 1420-1421.

[43] T. J. Fisher, P. H. Dussault, *Tetrahedron* **2017**, *73*, 4233-4258.

[44] M. T. Nunez, V. S. Martin, *The Journal of Organic Chemistry* **1990**, *55*, 1928-1932.

[45] A. K. Chakraborti, U. R. Ghatak, *Synthesis* **1983**, *1983*, 746-748.

[46] S.-I. Murahashi, N. Komiya, Y. Oda, T. Kuwabara, T. Naota, *The Journal of Organic Chemistry* **2000**, *65*, 9186-9193.

[47] S. Chen, Z. Liu, E. Shi, L. Chen, W. Wei, H. Li, Y. Cheng, X. Wan, *Organic Letters* **2011**, *13*, 2274-2277.

[48] J. Hu, D. Zhang, F. W. Harris, *The Journal of Organic Chemistry* **2005**, *70*, 707-708.

[49] S. K. Gupta, J. Choudhury, *ChemCatChem* **2017**, *9*, 1979-1984.

[50] C. S. Yi, K.-H. Kwon, D. W. Lee, *Organic Letters* **2009**, *11*, 1567-1569.

[51] S. Ranganathan, K. M. Muraleedharan, P. Bharadwaj, K. P. Madhusudanan, *Chemical Communications* **1998**, 2239-2240.

[52] J. Wei, X. Jia, J. Yu, X. Shi, C. Zhang, Z. Chen, *Chemical Communications* **2009**, 4714-4716.

[53] D. Yang, C. Zhang, *The Journal of Organic Chemistry* **2001**, *66*, 4814-4818.

[54] M. Farina, G. Audisio, *Tetrahedron* **1970**, *26*, 1839-1844.

[55] I. W. C. E. Arends, T. Kodama, R. A. Sheldon, in *Ruthenium Catalysts and Fine Chemistry: -/-* (Eds.: C. Bruneau, P. H. Dixneuf), Springer Berlin Heidelberg, Berlin, Heidelberg, **2004**, pp. 277-320.

[56] B. Plietker, *The Journal of Organic Chemistry* **2003**, *68*, 7123-7125.

[57] B. Plietker, M. Niggemann, *Organic Letters* **2003**, *5*, 3353-3356.

[58] G. J. Bhatt, P. T. Deota, D. Upadhyay, P. K. Jha, *RSC Advances* **2021**, *11*, 34498-34502.

[59] M. Caricato, M. J. Frisch, J. Hiscocks, M. J. Frisch, *Gaussian 09: IOps Reference*, Gaussian, **2009**.

[60] A. D. Becke, *Physical Review A* **1986**, *33*, 2786-2788.

[61] W. P. Griffith, in *Ruthenium Oxidation Complexes: Their Uses as Homogenous Organic Catalysts* (Ed.: W. P. Griffith), Springer Netherlands, Dordrecht, **2011**, pp. 1-134.

2.8 Spectral data of compounds

2.8.1 *^{1}H and ^{13}C NMR spectra and HRMS of products*

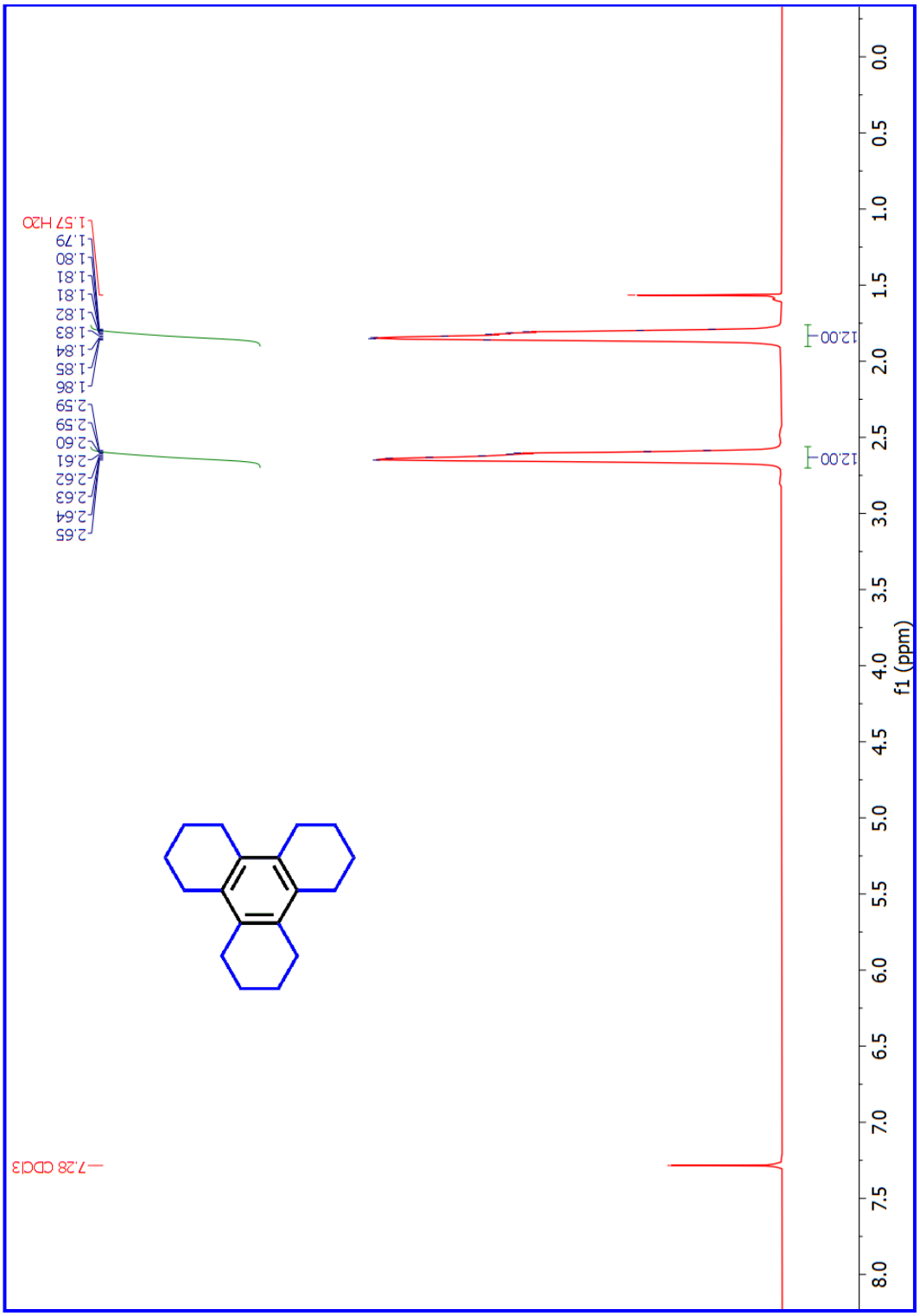

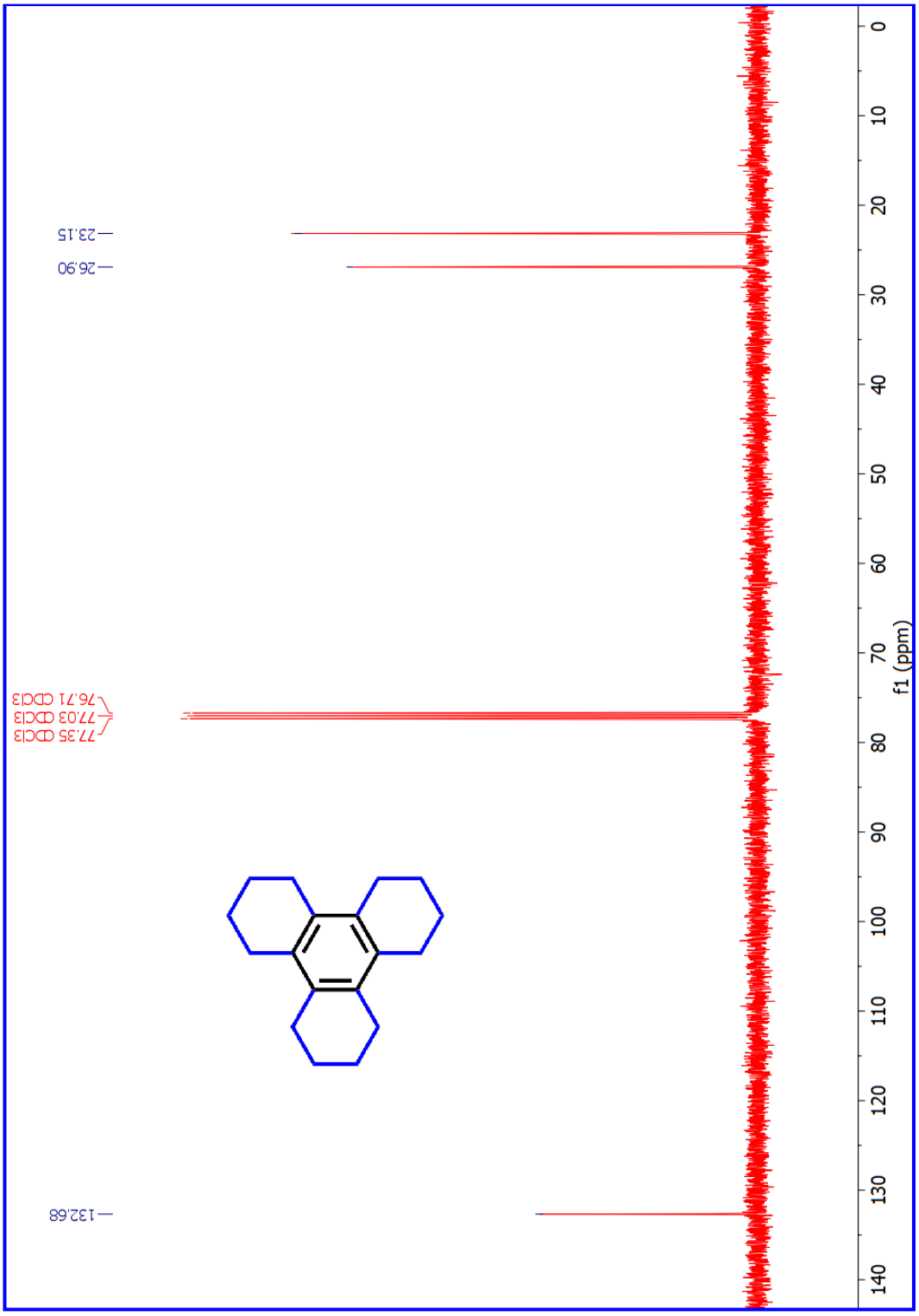
23.15
26.90
77.35 CDCl3
77.03 CDCl3
76.71 CDCl3
132.68
f1 (ppm)

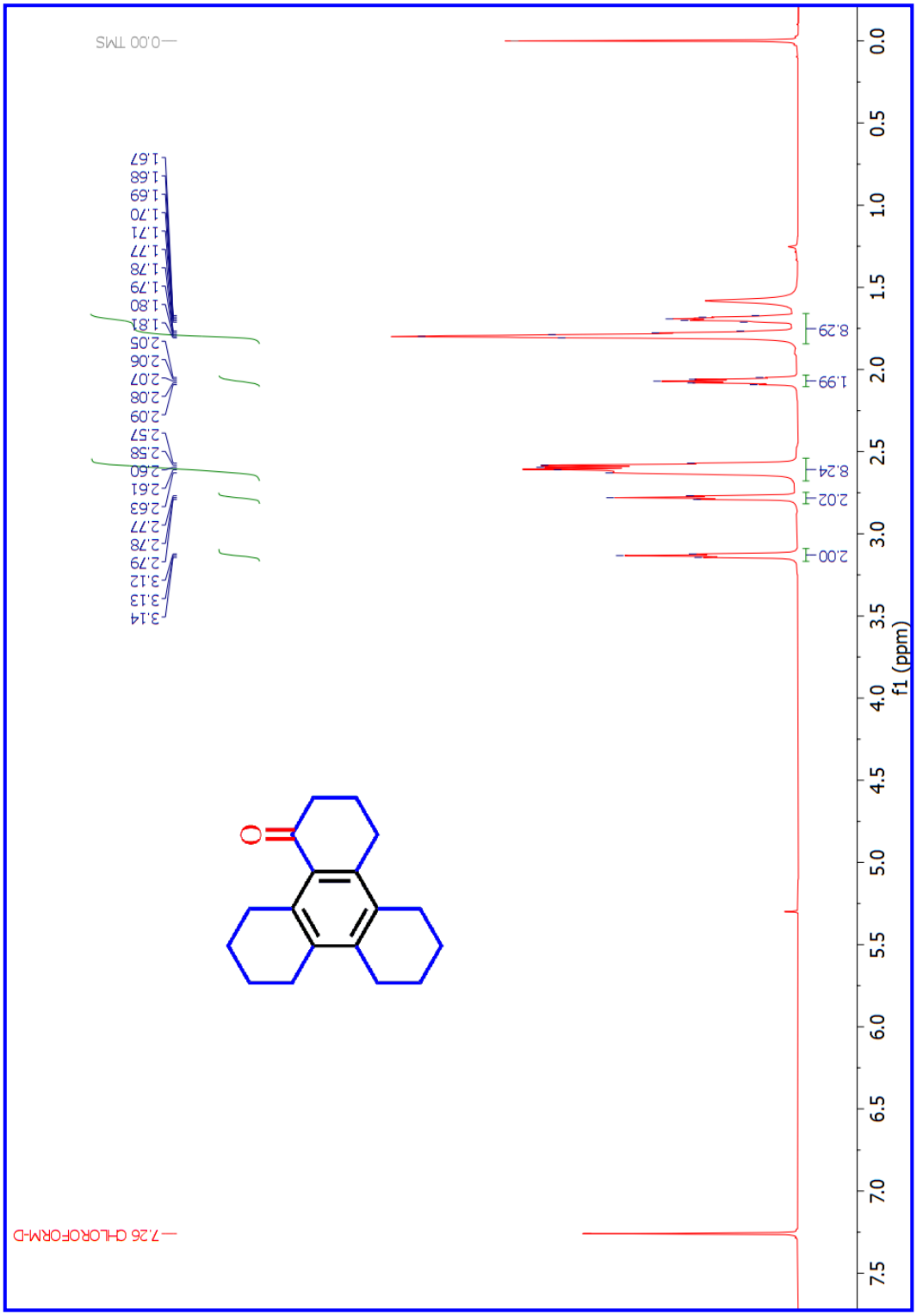
0.00 TMS
7.26 CHLOROFORM-D
1.67
1.68
1.69
1.70
1.71
1.77
1.78
1.79
1.80
1.81
2.05
2.06
2.07
2.08
2.09
2.57
2.58
2.60
2.61
2.63
2.77
2.78
2.79
3.12
3.13
3.14
8.29
1.99
8.24
2.02
2.00
O
f1 (ppm)

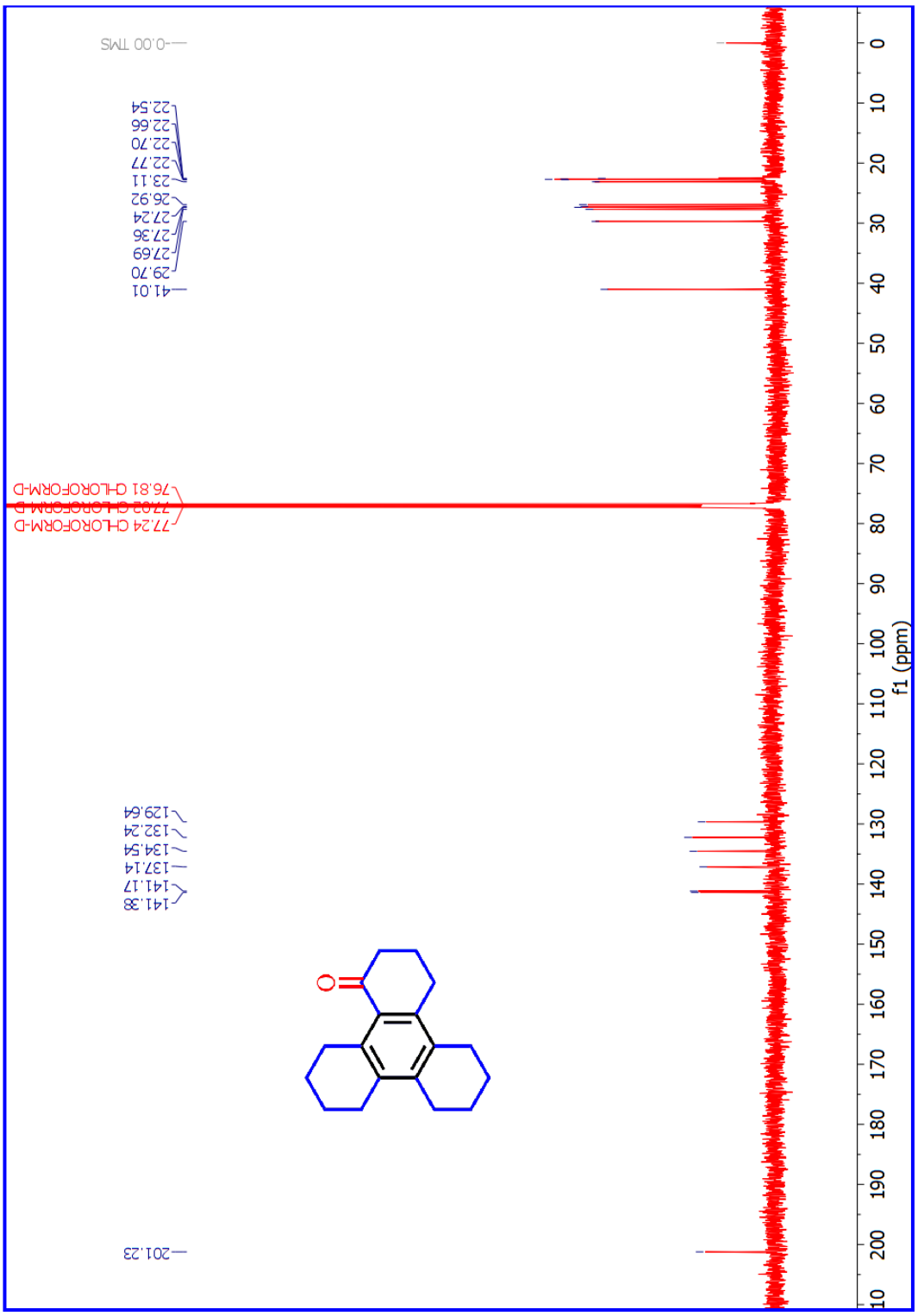
0.00 TMS
22.54
22.66
22.70
22.77
23.11
26.92
27.24
27.36
27.69
29.70
41.01
76.81 CHLOROFORM-D
77.02 CHLOROFORM-D
77.24 CHLOROFORM-D
129.64
132.24
134.54
137.14
141.17
141.38
201.23
f1 (ppm)

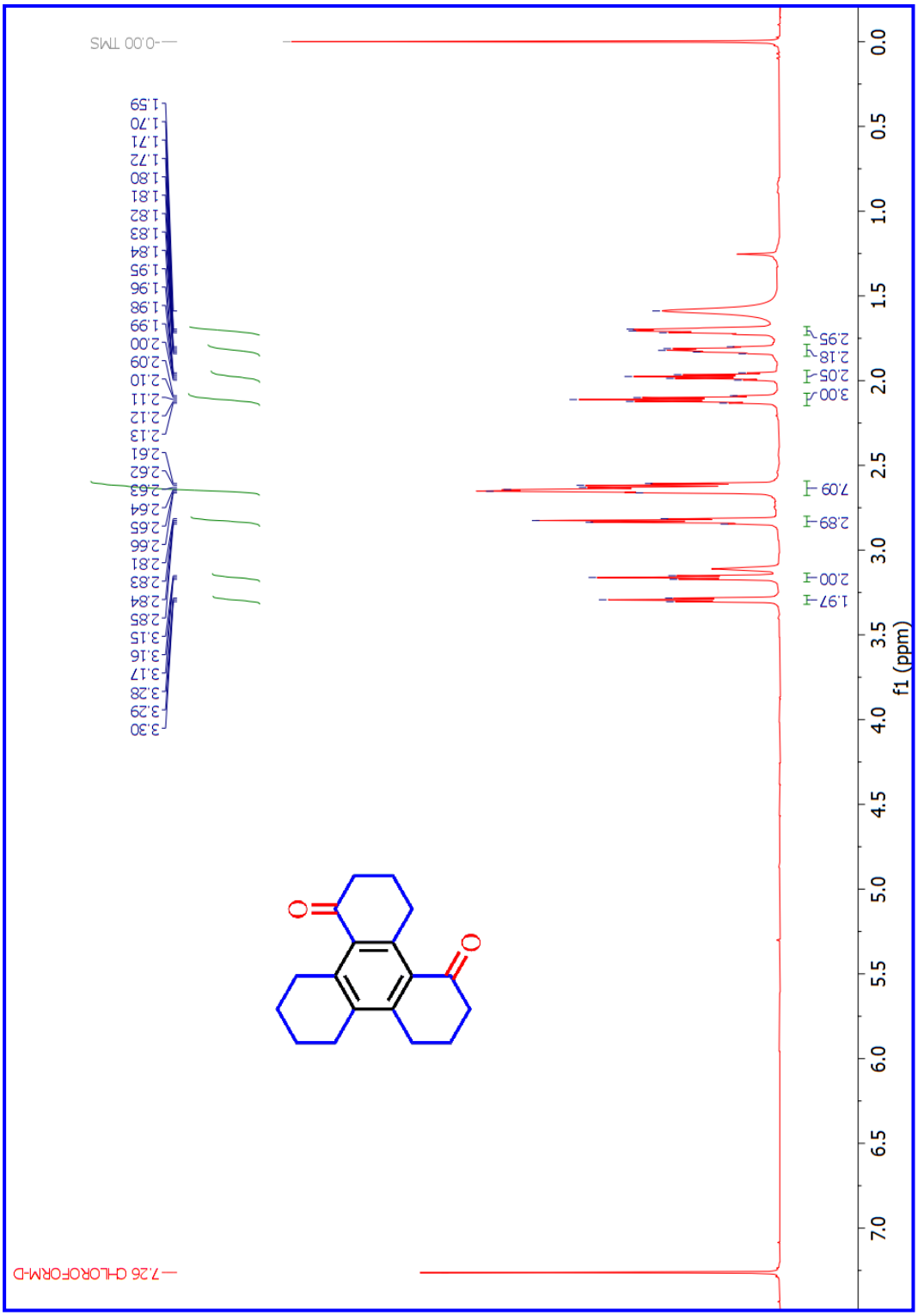
0.00 TMS
7.26 CHLOROFORM-D
1.59
1.70
1.71
1.72
1.80
1.81
1.82
1.83
1.84
1.95
1.96
1.98
1.99
2.00
2.09
2.10
2.11
2.12
2.13
2.61
2.62
2.63
2.64
2.65
2.66
2.81
2.83
2.84
2.85
3.15
3.16
3.17
3.28
3.29
3.30
2.95
2.18
2.05
3.00
7.09
2.89
2.00
1.97
f1 (ppm)

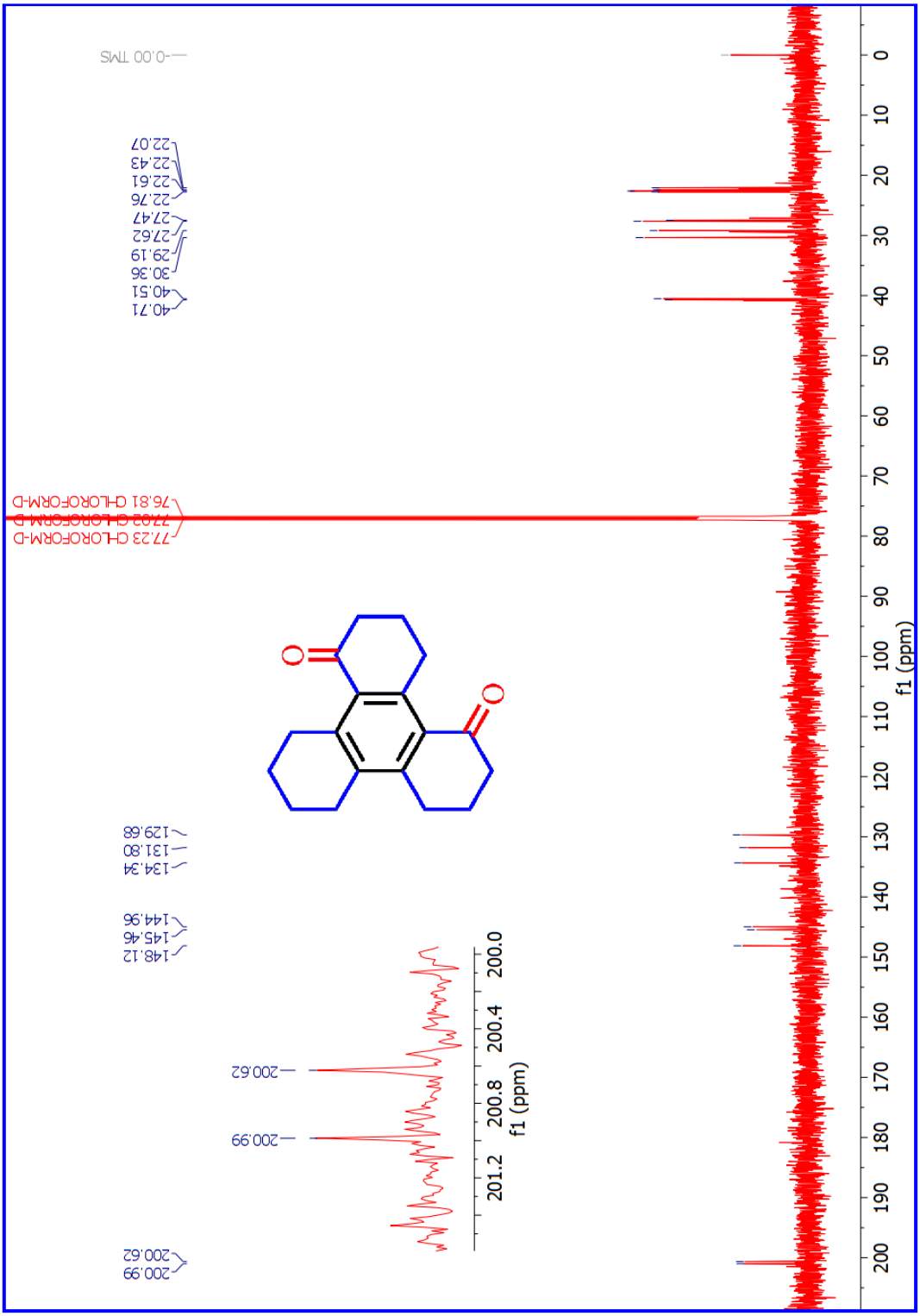
0.00 TMS
22.07
22.43
22.61
22.76
27.47
27.62
29.19
30.36
40.51
40.71
76.81 CHLOROFORM-D
77.02 CHLOROFORM-D
77.23 CHLOROFORM-D
129.68
131.80
134.34
144.96
145.46
148.12
200.62
200.99
f1 (ppm)

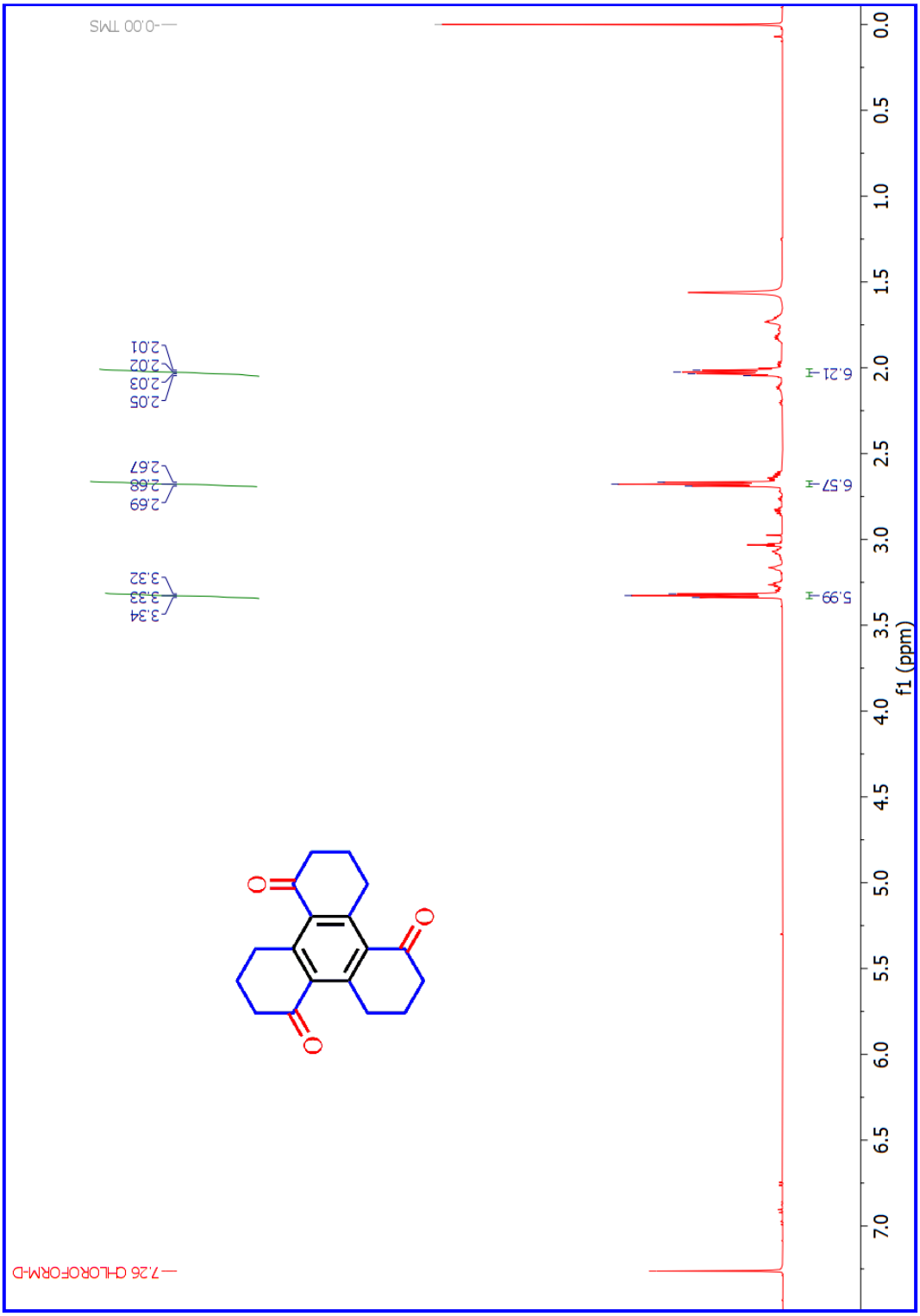
TMS 0.00
CHLOROFORM-D 7.26
6.21
6.57
5.99
2.01
2.02
2.03
2.05
2.67
2.68
2.69
3.32
3.33
3.34
f1 (ppm)

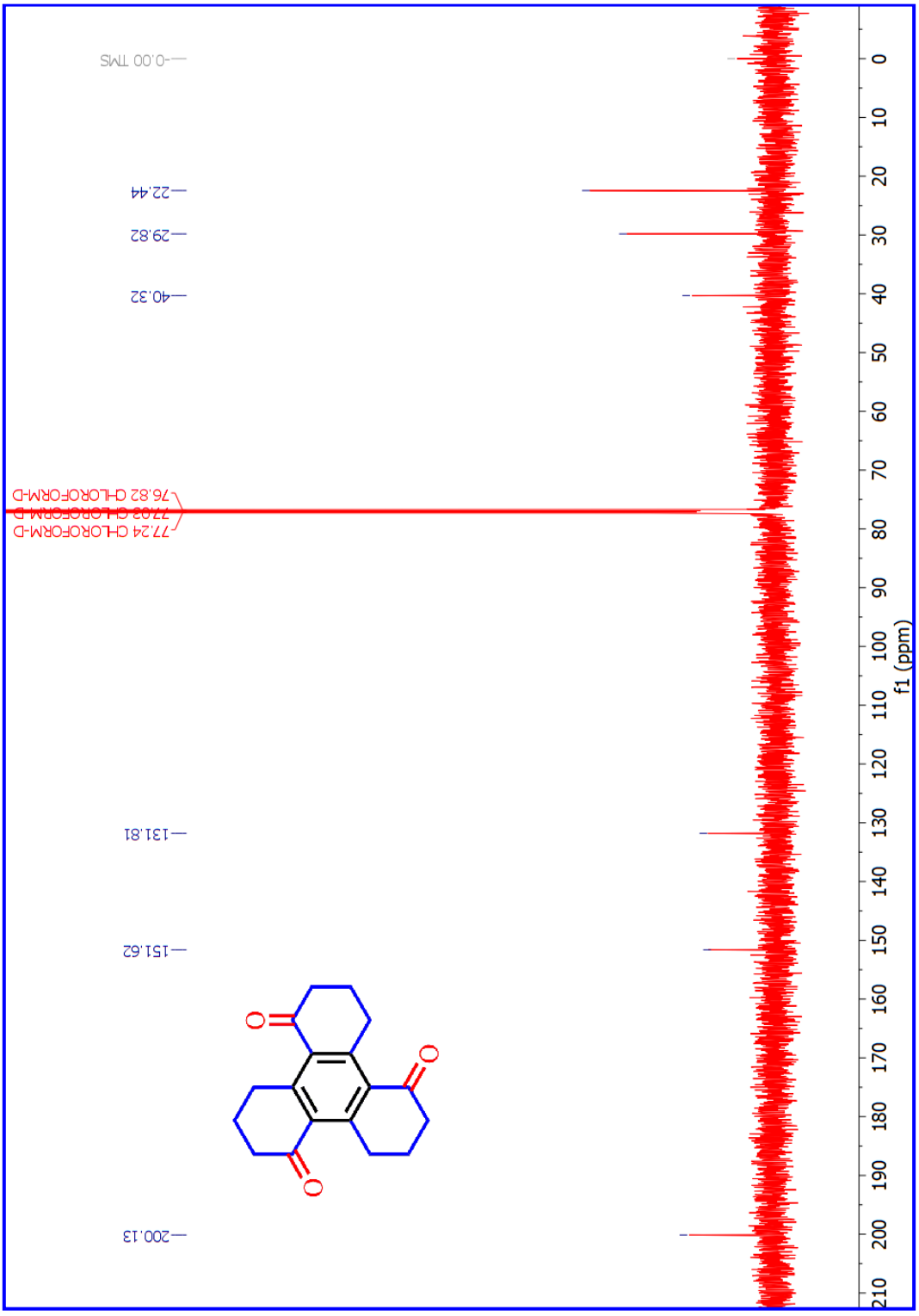
0.00 TMS
22.44
29.82
40.32
76.82 CHLOROFORM-D
77.02 CHLOROFORM-D
77.24 CHLOROFORM-D
131.81
151.62
200.13
f1 (ppm)

Elemental Composition Report

Single Mass Analysis

Tolerance = 5.0 PPM / DBE: min = -1.5, max = 50.0
Element prediction: Off
Number of isotope peaks used for i-FIT = 5

Monoisotopic Mass, Even Electron Ions
72 formula(e) evaluated with 1 results within limits (up to 50 best isotopic matches for each mass)
Elements Used:
C: 11-25 H: 10-30 N: 0-2 O: 0-8 Na: 0-1

Sample Name : GB026
Test Name : HRMS-1
020320-GB026 93 (0.883)

IITRPR

XEVO G2-XS QTOF

1: TOF MS ES+
1.72e+008

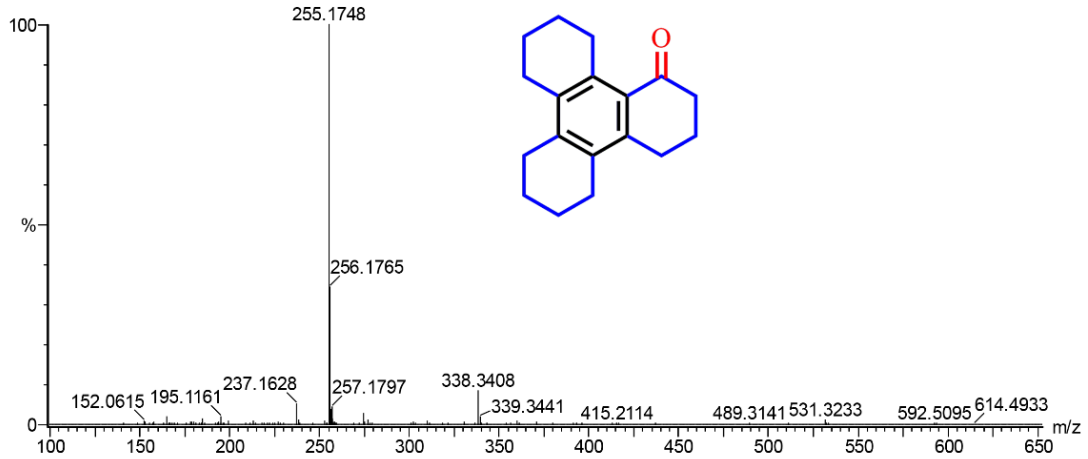

Minimum:				-1.5				
Maximum:		5.0	5.0	50.0				
Mass	Calc. Mass	mDa	PPM	DBE	i-FIT	Norm	Conf(%)	Formula
255.1748	255.1749	-0.1	-0.4	7.5	2329.6	n/a	n/a	C18 H23 O

Elemental Composition Report **Page 1**

Single Mass Analysis
Tolerance = 20.0 PPM / DBE: min = -1.5, max = 50.0
Element prediction: Off
Number of isotope peaks used for i-FIT = 5

Monoisotopic Mass, Even Electron Ions
9 formula(e) evaluated with 1 results within limits (up to 50 best isotopic matches for each mass)
Elements Used:
C: 11-25 H: 10-30 O: 0-4

Sample Name : GB027 IITRPR XEVO G2-XS QTOF
Test Name : HRMS-1
020320-GB027 23 (0.237) 1: TOF MS ES+
5.55e+007

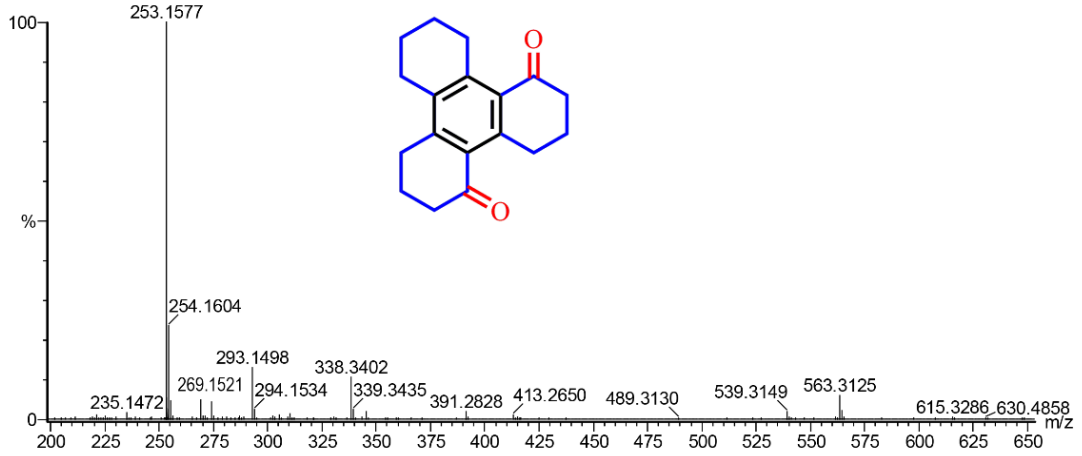

Minimum:				-1.5				
Maximum:		5.0	20.0	50.0				
Mass	Calc. Mass	mDa	PPM	DBE	i-FIT	Norm	Conf(%)	Formula
269.1521	269.1542	-2.1	-7.8	8.5	1519.8	n/a	n/a	C18 H21 O2

Elemental Composition Report **Page 1**

Single Mass Analysis
Tolerance = 20.0 PPM / DBE: min = -1.5, max = 50.0
Element prediction: Off
Number of isotope peaks used for i-FIT = 5

Monoisotopic Mass, Even Electron Ions
8 formula(e) evaluated with 1 results within limits (up to 50 best isotopic matches for each mass)
Elements Used:
C: 11-25 H: 10-30 O: 0-4

Sample Name : GB028
Test Name : HRMS-1
020320-GB028 21 (0.220)

IITRPR

XEVO G2-XS QTOF

1: TOF MS ES+
7.35e+007

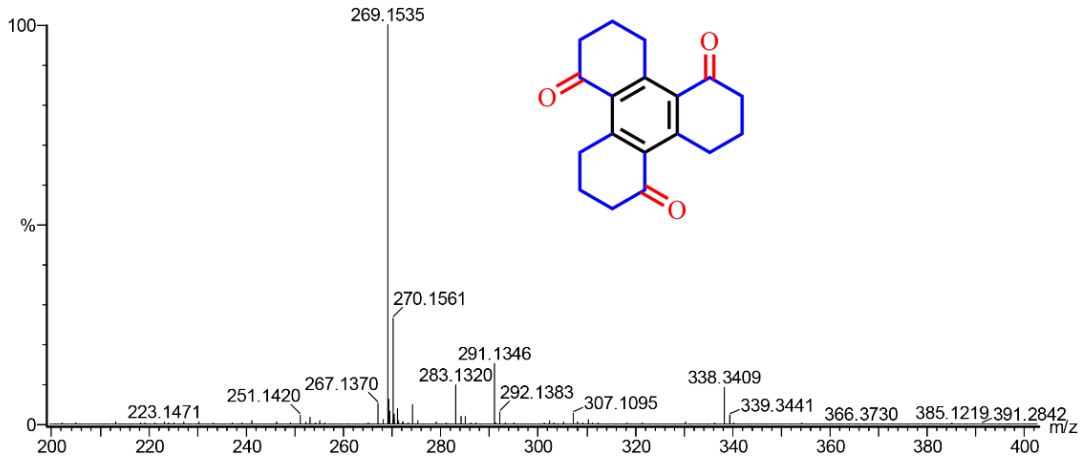

Minimum:				-1.5				
Maximum:		5.0	20.0	50.0				
Mass	Calc. Mass	mDa	PPM	DBE	i-FIT	Norm	Conf(%)	Formula
283.1320	283.1334	-1.4	-4.9	9.5	1622.7	n/a	n/a	C18 H19 O3